ANKARA YILDIRIM BEYAZIT UNIVERSITY

GRADUATE SCHOOL OF NATURAL AND APPLIED SCIENCES

DESIGN OPTIMIZATION OF A DIRECT RADIO FREQUENCY SAMPLING MULTI-GNSS RECEIVER FRONT END

M.Sc. Thesis by

Ahmed Eltayeb Ahmed ELBUSHRA

Department of Electrical and Electronic Engineering

January, 2023

ANKARA

DESIGN OPTIMIZATION OF A DIRECT RADIO FREQUENCY SAMPLING MULTI-GNSS RECEIVER FRONT END

A Thesis Submitted to

The Graduate School of Natural and Applied Sciences of

Ankara Yıldırım Beyazit University

In Partial Fulfillment of the Requirements for the Degree of Master of Science in Electrical and Electronic Engineering, Department of Electrical and Electronic Engineering

By

Ahmed Eltayeb Ahmed ELBUSHRA

January, 2023

ANKARA

M.Sc. THESIS EXAMINATION RESULT FORM

We have read the thesis entitled **"DESIGN OPTIMIZATION OF A DIRECT RADIO FREQUENCY SAMPLING MULTI-GNSS RECEIVER FRONT END"** completed by **AHMED ELTAYEB AHMED ELBUSHRA** under the supervision of **PROF. DR. ALAADEEN ELROUBY** and we certify that in our opinion it is fully adequate, in scope and in quality, as a thesis for the degree of Master of Science.

Prof. Dr. ALAADEEN ELROUBY

Supervisor

Assoc. Prof. ENVER ÇAVUŞ

Jury Member

Asst. Prof. Dr. Mehmet Efe ÖZBEK

Jury Member

Prof. Dr. Sadettin ORHAN

Director

Graduate School of Natural and Applied Sciences

ETHICAL DECLARATION

I hereby declare that, in this thesis which has been prepared in accordance with the Thesis Writing Manual of Graduate School of Natural and Applied Sciences,

- All data, information and documents are obtained in the framework of academic and ethical rules,
- All information, documents and assessments are presented in accordance with scientific ethics and morals,
- All the materials that have been utilized are fully cited and referenced,
- No change has been made on the utilized materials,
- All the works presented are original,

and in any contrary case of above statements, I accept to renounce all my legal rights.

Date:2023,6January **Signature: …….....**

Name & Surname: AHMED ELTAYEB AHMED ELBUSHRA

ACKNOWLEDGMENTS

First and above all, I would like to thank the almighty Allah for bestowing his blessings on me and offering me the strength to carry out and complete this work.

I would like to express my sincere gratitude to my supervisor, **Prof. Dr. Alaa EL-ROUBY** for his tremendous support and motivation during my study. His immense knowledge and precious recommendations constituted the milestones of this study. His guidance assisted me all the time of my research and while writing this thesis. I am also very grateful to the members of my thesis committee, **Assoc. Prof. ENVER ÇAVUŞ** and **Asst. Prof. Dr. Mehmet Efe ÖZBEK** for their consideration, support, and helpful advice.

I would like to express my special thanks to my parents, my brothers and my sister for their encouragement, patience, and love. It would have been impossible for me to complete this work without their support, inspiration and understanding. Finally, my heartfelt gratitude to all those who helped me in completing this work.

DESIGN OPTIMIZATION OF A DIRECT RADIO FREQUENCY SAMPLING MULTI-GNSS RECEIVER FRONT END

ABSTRACT

The recent development in satellite navigation systems is experiencing a meteoric rise with the releases of the European and Chinese systems, and its already competing with the existing American and Russian positioning systems. GNSS receivers will have to adapt to a multitude of signals at different frequencies or from different constellations. To achieve that in a traditional way, several receivers front-ends are required for each GNSS receiver. This approach quickly becomes complex and expensive for multi-frequency receivers. A new and elegant approach is proposed to overcome this issue by using direct RF sampling technique that samples all signals simultaneously and process them digitally afterwards. This approach greatly reduces the hardware requirement in the traditional receiver by placing the analog to digital converter as close as possible to the antenna and eliminating the mixer (analog RF) stages. The lack of theoretical contribution in the literature has been the main motive for this study.

The thesis aims to introduce a complete theoretical framework on direct sampling RF receiver, followed by simulation and correlation between theoretical and simulation results.

A part of the theoretical framework, a new approach of a simplified sampling frequency selection algorithms is proposed for the single and multiple bands while as well as analyzing and modeling the relationship between system noise and the sampling frequency.

In the simulation part, a DRFS receiver for the GPS L1 C/A signal is considered. The RF Filters limits the signal capture with band of 15 MHz around the L1 Frequency. Finally, The sampling stage is done using a several sampling frequencies of ($30.1217\ MHz$, $90.365\ MHz$, $203.321\ MHz$) followed by correlations to verify the effect of the sampling frequency on the RF signal spectrum as well as the system noise.

Keywords: GNSS, satellite navigation, GPS, Direct RF sampling, noise folding

DOĞRUDAN RADYO FREKANSI ÖRNEKLEMELİ ÇOKLU GNSS ALICI ÖN UCUNUN TASARIM OPTİMİZASYONU (TR)

ÖZ

Uydu navigasyon sistemlerindeki son gelişmeler, Avrupa ve Çin sistemlerinin piyasaya sürülmesiyle meteorik bir yükseliş yaşıyor ve halihazırda mevcut Amerikan ve Rus konumlandırma sistemleriyle rekabet ediyor. GNSS alıcıları, farklı frekanslardaki veya farklı takımyıldızlarından gelen çok sayıda sinyale uyum sağlamak zorunda kalacaktır. Bunu geleneksel bir şekilde başarmak için, her bir GNSS alıcısı için, birkaç alıcı ön yüz gerekir. Bu yaklaşım, çok frekanslı alıcılar için hızla karmaşık ve pahalı hale gelir. Tüm sinyalleri aynı anda örnekleyen ve daha sonra dijital olarak işleyen doğrudan RF örnekleme tekniği kullanılarak bu sorunun üstesinden gelmek için yeni ve verimli bir yaklaşım önerilmiştir. Bu yaklaşım, analog-dijital dönüştürücüyü, antene mümkün olduğunca yakın yerleştirerek ve mikser (analog RF) aşamalarını ortadan kaldırarak, geleneksel alıcıdaki donanım gereksinimini büyük ölçüde azaltır. Literatürde, teorik katkının olmaması bu çalışmanın temel nedeni olmuştur. Tez, doğrudan örneklemeli RF alıcısı hakkında eksiksiz bir teorik çerçeve sunmayı, ardından, teorik ve simülasyon sonuçları arasındaki simülasyonu ve korelasyonu sunmayı amaçlamaktadır.

Teorik çerçevenin bir parçası olarak, sistem gürültüsü ve örnekleme frekansı arasındaki ilişkinin analiz edilmesi ve modellenmesinin yanı sıra, tekli ve çoklu bantlar için basitleştirilmiş bir örnekleme frekansı seçim algoritmalarına yönelik, yeni bir yaklaşım önerilmiştir.

Simülasyon bölümünde, GPS L1 C/A sinyali için bir DRFS alıcısı ele alınmıştır. RF Filtreleri, sinyal yakalamayı L1 Frekansı civarında 15 MHz bantla sınırlar. Son olarak, örnekleme aşaması, (30.1217 MHz, 90.365 MHz, 203.321 MHz) birkaç örnekleme frekansı ve ardından örnekleme frekansının sistem gürültüsünün yanı sıra RF sinyal spektrumu üzerindeki etkisini doğrulamak için korelasyonlar kullanılarak yapılır.

Anahtar Kelimeler: GNSS, uydu navigasyonu, GPS, Doğrudan RF örnekleme, gürültü katlama

CONTENTS

NOMENCLATURE

Abbreviations

BW	Bandwidth
DRFS	Direct Radio Frequency Sampling
GNSS	Global Navigation Satellite System
GA	Ground Antennas
LNA	Low Noise Amplifier
MCS	Master Control Stations
MS	Monitoring Stations
RMS	Root Mean Square
SNR	Signal to Noise Ratio
SDR	Software Defined Radio

LIST OF TABLES

LIST OF FIGURES

CHAPTER 1

INTRODUCTION

Global Navigation Satellite Systems (GNSS) is considered one of the most promising space systems. GNSS consists of a constellation of Earth-orbiting satellites that are used to provide a global coverage by broadcasting their location and timing data from space to GNSS receivers, which use this data to determine their (the receivers) locations. Currently GNSS includes four main global systems that offer full coverage which are GPS, GLONASS, Galileo and Bei Dou beside other regional systems. GNSS plays a critical role in many applications like tracking/mapping devices, industrial machinery, sea vessels, automobiles, and air navigations [1].

GNSS receivers are used to amplify and filter signals of interest then use them to calculate the ground position by trilateration[2]. GNSS receivers can be divided into 3 major blocks; The antenna, RF front-end and the software subsystems as shown in

Figure **1.1** [3]. The RF front-end is used to realize four basic functions which are:

- Amplification of the signals of interest to compensate for the losses incurred during transmission.
- Bandpass Filter (BPF) to prevent out of band signals from saturating the input stages or interfere with the signal of interest.
- Direct down converting the desired signal (F_c) to a target intermediate frequency (F_{IF}) using bandpass sampling in direct rf receiver (DRFS) or a mixer in other architectures.
- Direct conversion of the signal of interest from analog to digital domain.

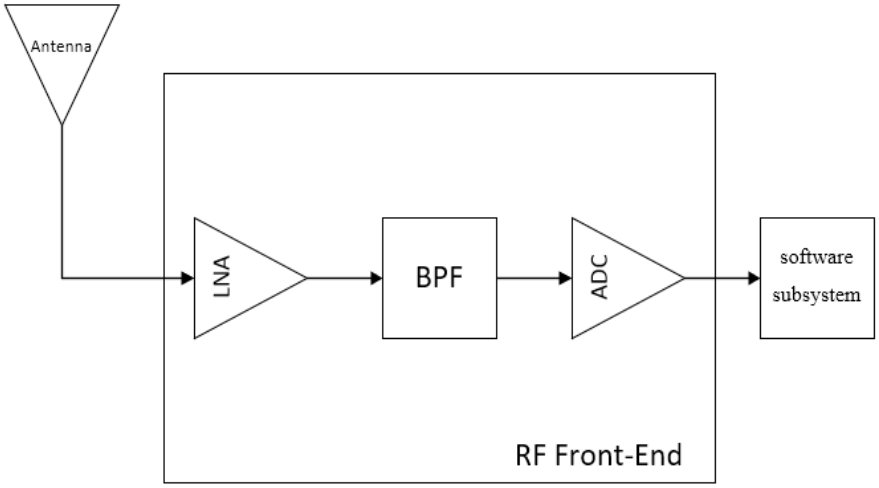

Figure 1.1 Front-End major blocks

In this part we will briefly describe a number of typical structures for GNSS receivers front end, it includes super-heterodyne, homodyne, low-IF, direct radio frequency sampling receivers and software defined radio, which will be explained in more details in CHAPTER 3.

Super-heterodyne receiver main principle is based on frequency mixing, which down-convert received signal of interest (F_c) to a specific intermediate signal (F_{IF}).These conversion stages can be single as shown in Figure 3.1 or dual conversion stages where the first state signal (F_c) is down converted to intermediate frequency (F_{IF}) and in second the stage it is from intermediate frequency (F_{IF}) to a near zero Hz intermediate frequency (F_{IF1}) signal as shown in Figure 3.2. Dual conversion stages are particularly beneficial for higher-frequency applications.

Homodyne receivers is the most widely used structure it convert the signal of interest (F_c) directly to baseband in a single stage as shown is Figure 3.4 hence they are called Direct IF architectures or Zero-IF architectures the down conversion operation must provide quadrature outputs to avoid loss of information. Single conversion homodyne is known to have less component and very simple.

Low-IF receiver structure as shown in Figure 3.5 has all the signals of interest converted to low-IF frequency which is then down-converted to baseband signal in digital domain. Low-IF architecture comprises the advantages of both heterodyne and homodyne receivers.

Direct RF sampling receiver Figure 1.2 started to gain a lot of attention due to the performance advancement in analog to digital converters (ADCs) in the past few years, it enabled us to directly digitize the signal of interest at radio frequencies using a ADC thereby replacing the receiver's analog components such as mixers, local oscillators, intermediate frequency filters and amplifiers This translates into a reduction in the cost of materials, size, power consumption, design time and weight, whilst enhancing the flexibility and software programmability of the entire system which would hardly be achieved with the traditional receivers.

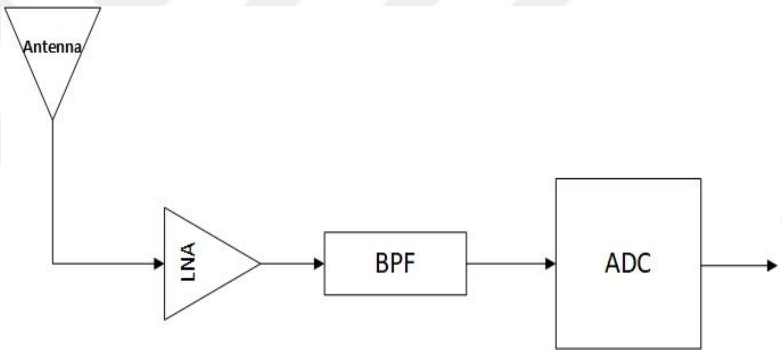

Figure 1.2 Single band GNSS Direct RF Sampling Receiver

The DRFS receiver has been compromised for some time because of the inordinate power consumption and undue requirements for the sampling process because of the high frequency signals to be sampled. However, some designers have come up with ADCs that can remedy the power consumption and sampling issues. Multi-GNSS DRFS Receiver collect multi-bands signal that are transmitted from satellites with multiple ranging signals and navigation data. The more signals the receiver can access, the more information it can collect from the satellites, the more accurate and reliable the computed position will be. The receiver in Figure 1.3 consist of multiple bandpass filters for multiple GNSS bands and then combined to be sampled and processed by the ADC.

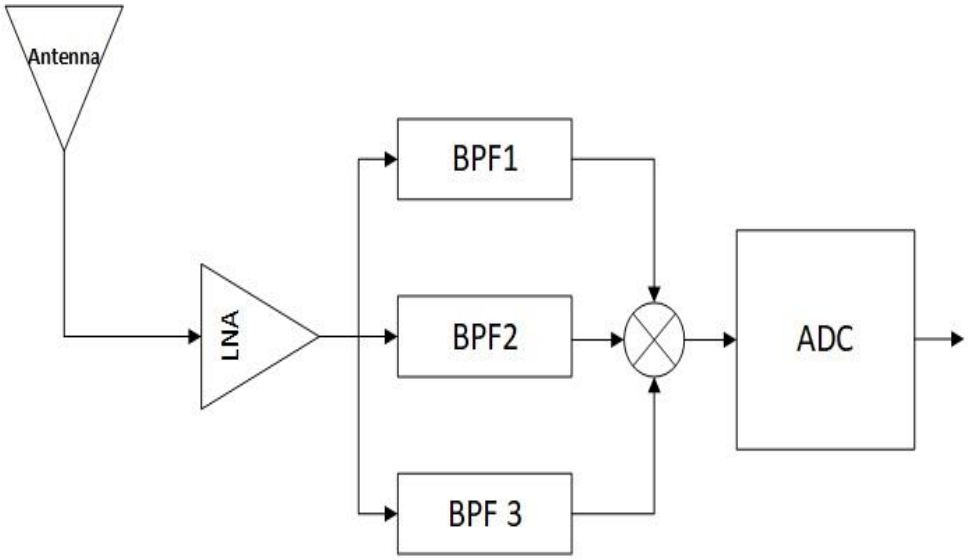

Figure 1.3 Multi-band GNSS Direct RF Sampling Receiver

1.1 Background and Motivation

The first Global Positioning Satellite (GPS) satellite was launched in 1978 by the United States with its multiple bands: L1, L2 and L5, since then several countries started the race to launch their own global navigation system; European Union (Galileo), Russia (GLONASS) and China (Bei Dou)[2]. These different systems result in a GPS receiver (Front-end and digital signal processing) not being fully compatible with the other systems that motivates us to develop a multi-GNSS receiver with a universal access to other systems.

Global Navigation Satellite System (GNSS) receiver designs has been evolving over the past three decades years. knowing that super heterodyne receiver is the most commercially used GNSS receiver that is available right now, therefore we would like to utilize the usage of the new developed direct radio frequency sampling receiver (DRFS) which require less components and significantly reduced in size, weight, cost, and power consumption, it meets the needs for higher precision, better satellite visibility, greater integrity, and more robustness for the standard user[2]. All these advantages can be a huge opportunity to seize and makes a multi-GNSS DRFS receiver a worthy contender in the commercial world. unfortunately, the main problem with DRFS architecture is the need for high quality sampling process with

more power consumption which will makes our signal prone to noise effects like noise folding and sampling jitter[2], all these effects will be explain in details throughout the thesis.

1.2 Thesis Contributions and Significance

The major contributions of the thesis are summarized below but will be explained in detail all along this document:

- A detailed Theoretical analysis of the critical parameters in the design of direct RF sampling multi-GNSS receiver like noise figure, dynamic range, and ADC noises (jitter sampling, quantization noise and noise folding).
- A detailed spectrum analysis of direct RF sampling multi-GNSS front-end is presented, it starts by deriving a general mathematical expression of the multi-band GPS signal, the expression is modeled as the summation of different GPS frequency bands (M), each band consist of specific carrier frequency (f_{cj}) like GPS bands; L1(f_{c1} = 1575.42 MHz) , L2 (f_{c2} = 1227.60 MHz) and L5($f_{c3} = 1176$ MHz). This general formula is modified in each stage (amplification, filtering, and ADC sampling) shown in the proposed direct RF sampling front-end block diagram in Figure 1.3.
- An optimized multi-band direct bandpass sampling algorithm is implemented and tested; it will provide a more flexible way in choosing the optimal sampling frequency of the ADC compared to previous literature work. The algorithm is tested on the GPS L bands (L1, L2 and L5) and it results in a list of sampling frequencies ranges that we can pick to obtain optimal performance. The algorithm is explained in detail in section3.9.
- Thorough analysis on the effects of noise figure and signal to noise ratio in direct multi- GNSS RF sampling receiver design with the mathematical derivations of each effect in section 3.9.3.
- Implementing and evaluating an optimized Design of a modern multi-GNSS receiver front-end using Direct radio frequency sampling architecture for GPS L1, L2 and L5 bands.

This thesis can be a source of literature for the overall research that is being undertaken today due to the continuous need for new technologies with greater capacity, reduced cost, and size as well as improved reliability that need to be employed for GNSS systems.

1.3 Scope

There is an upsurge of research interests in a Direct Radio Frequency Sampling (DRFS) receiver in pursuit for new technologies with greater capacity, reduced cost and size as well as improved reliability of communication systems[2]. The research has been substantial in applications such as VHF Radio, Radar Systems, Aircraft Communication and Address Reporting Systems (ACARS) and Emergency Locator Transmitters (ELTs)[4,5]. s

1.4 Thesis Outline

The thesis is organized in five chapters; chapter one gives an introduction where background information as well as the significance, motivation, and scope of the research are given. Chapter two explains the basics of Global Navigation for Satellite System (GNSS), their architecture, location positioning concepts and their global/regional systems. Chapter three expounds on the different receiver architectures where the working principle, advantages, and challenges of the super-heterodyne, homodyne, low IF and DRFS receivers are thoroughly presented. Chapter four elaborate the front-end design considerations for multi-GNSS DRFS receiver. Those design considerations include noise figure, sensitivity, selectivity as well as the ADC design and sampling requirements. Chapter five discusses findings, analyzes results and suggests future research points.

CHAPTER 2

BASICS OF GNSS

2.1 Introduction

Global Navigation Satellite System is a satellite system that is used to find the geographical location of a specific user with global coverage, by utilizing the constellations of satellites to transmit radio-coded wave signals from space at precise times. Since those coded signals travel at the speed of light we can approximate the time it takes for each signal to travel from the GNSS satellite to the user's receiver. Using Eq. (2.1). we can find the d distance using c the speed of light and t transmit time:

$$c = q * t \quad \textbf{(2.1)}$$

After measuring all the distances of all satellites that transmitted the coded signals, the user's receiver will be able to calculate its own position (longitude, latitude, and altitude) using the concept of trilateration as explained in section 2.3.1. The performance of GNSS is evaluated based on four criteria:

- Accuracy: the difference between user's receiver measured and real position speed, or time.
- Integrity: it's the capacity to provide a threshold of confidence and, in the event of an anomaly in the positioning data, an alarm.
- Continuity: it's the ability of the system to function without interference.
- Availability: the percentage of time a signal satisfies the previous criteria.

Currently, GNSS consist of four main satellite technologies in the world that are fully operational and provide high accuracy and guaranteed global positioning services under civilian control these technologies are NAVSTAR that provide Global Positioning System (GPS) services by the United States, GLONASS by the Russians,

Galileo Positioning System made by the European Union, Bei Dou Global Navigation System and Additionally, there are two regional systems – Japanese QZSS and Indian IRNSS or NavIC[6,7]. This chapter is going to explore GPS and its features in detail.

2.2 GNSS System Architecture

The GNSS system mainly consists of three main segments: the space segment, which compares the satellites; the control segment (also known as the ground segment); which monitors the satellites and their operation; the user segment; which measure positioning, velocity, and the exact time to users using GNSS receivers, as shown in Figure 2.1**.**

2.2.1 GNSS Segmentations

2.2.1.1 Space Segment

The main functions of the space segment are to transmit coded navigation signals and to store and retransmit the navigation message sent by the control segment (explained in section). Highly stable atomic clocks onboard the satellites are used to control all these transmissions. The space segment consists of the full constellation of satellites where its set up to have at least four satellites in view by the users from any point on the planet. The GPS system has 27 satellites in the orbits which ensures global coverage at all times, with a few extra satellites to increase GPS performance but they are not part of the core constellation, by including the extras makes a total of 30 GPS satellites. The satellites are placed in a Medium Earth Orbit (MEO), at an altitude of 20200km an inclination of 55° relative to the equator, and each satellite circles the earth twice a day[8,9]. When it comes to other satellite systems, currently there are 27 GLONASS, 18 Galileo, and 20 BeiDou satellites in the orbits [10]. The satellites are responsible for generating the coded navigation signals, for example in GPS system it is carrying stable clocks, and the signal L1(1575.42MHz) that include the coarse acquisition (C/A) code with encryption code P(Y) code to authorize users the GPS satellites also carry L2 (1227.60MHz) that include the precision P (Y) code

for correcting the ionospheric propagation delays, section 2.5 can expand on signal characteristics more [10].

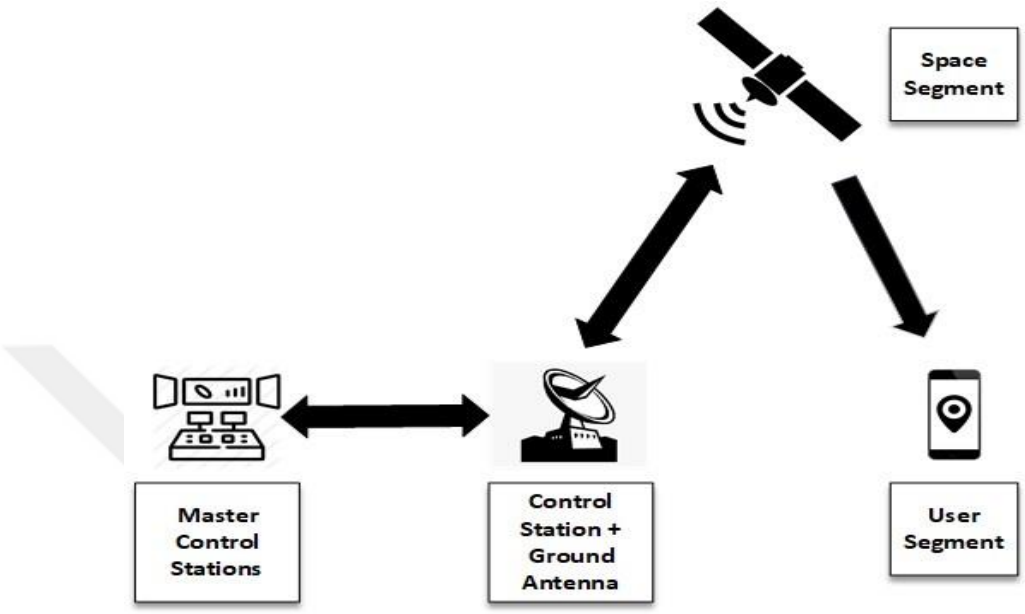

Figure 2.1 GNSS system architecture

2.2.1.2 Control Segment

The control segment (known as the ground segment) overseas the GNSS systems operation, its main functions are:

- Monitor and maintain the satellite constellation status and configurations.
- predict ephemeris and satellite clock evolution.
- Maintain the GNSS time scale (using atomic clocks)
- send information of estimated orbits and time information to the satellites in the navigation messages.

The control segment consists of Master Control Stations (MCS), several Monitoring Stations (MS), and the Ground Antennas (GA).

The Master Control Stations (MCS) is considered to be the fundamental part of the control segment, it is superintended for monitoring providing command, control, and maintenance services to the space segment operating system.

Monitoring Stations (MS) are responsible show the specific information and data such as altitude, position, speed, and overall health of the orbiting satellites; all this collected data are sent to the Master Control Stations (MCS) to generate the navigation message after estimating the satellite orbits (ephemerides) and clock errors, and other variables.

Ground Antennas (GA) transmit the collected data obtain from MCS and MS within the navigation message to the satellite via S-band radio signals[9].

2.2.1.3 User Segment

The user segment consists of GNSS receivers with internal antennas and digital clocks. Their main functions are to receive the GNSS signal then determine pseudo-ranges (and other parameters) and calculate the geographical coordinates (longitude, latitude, and altitude) with high accuracy and time, these parameters are obtained by processing the information received within the GNSS signal [9].

GPS uses two calculations in the segment. The first one is for pseudo-range which measures the time difference between the satellites and the receiver by comparing the GPS received C/A and P(Y) codes which contain the timestamp (along with other parameters) of transmission from the satellite and the code containing the receiving time (along with other parameters) that is generated by the receiver itself. The second one is for carrier phase calculations which compare the phase difference between the received carrier signal and locally generated signal by the receiver at the same frequency [11].

2.3 GNSS Positioning Techniques

2.3.1 Concept of Trilateration

Trilateration is used to find the position of the user on earth once we know the location of exactly three satellites orbiting earth and their distance from your location

using equation (2.1). they can be found because satellites send out electromagnetic signals constantly which contain the time signals were sent. Each distance measurement to the satellites forms a sphere If the receiver detects a signal from only one satellite, we can tell that the user could be anywhere on the surface of a sphere of radius equal to the calculated distance from the satellite. When the user receives signals from two satellites (satellites 1 and 2), we could tell that the user is somewhere along the circle drawn by the intersections of the spheres described by the two signals. But when using a third satellite signal, we can tell the exact location of our device, because the three spheres will intersect in one point only. We can simplify this concept in 2D, using circles rather than spheres as shown in Figure 2.2 [10,12].

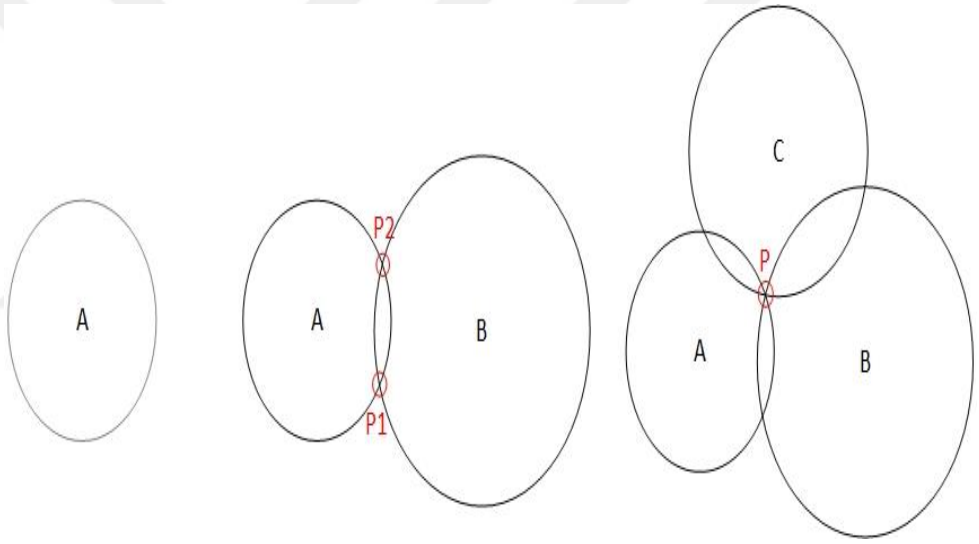

Figure 2.2 Satellites 2D/3D trilateration concept

The trilateration concept is fallible because in practice several errors could accrue in the distance calculations, to minimize this error percentage we need to consider the clocks involved in the process knowing they are not synchronized because time is considered an important factor in distance calculation as shown in equation **(2.1)**. There are three clock types involved:

- GNSS system clock.
- Satellite clocks.

- User receiver clock.

The GNSS system clock is used in the control stations (CS) on earth, they are the most accurate with a very high precision system.

the satellite clocks are one of the most critical components to obtain a high accuracy and stability clock we provide the satellites with high stability atomic oscillators. Despite this they accumulate certain time biases(offsets) and frequency drifts over time. These offsets and drifts are constantly estimated by the ground segment then the error percentage is minimized using correction terms.

The user's clocks are the most inaccurate and cheapest because typically they use crystal oscillators because the market needs these devices to be cheap and affordable[9].

2.3.2 Multilateration

This concept expands on trilateration with determining the user's location anywhere on earth by knowing at least four satellites and their distance from the user's receiver. The receiver A can calculate the location by solving four equations with four unknowns (X, Y, Z) and clock receiver clock bias where each equation corresponds to a specific satellite; the four equations analytical solution is written below:

$$R_A^1(t) = \sqrt{(X^1(t) - X_A)^2 + (Y^1(t) - Y_A)^2 + (Z^1(t) - Z_A)^2} + c.\Delta\delta$$

$$R_A^2(t) = \sqrt{(X^2(t) - X_A)^2 + (Y^2(t) - Y_A)^2 + (Z^2(t) - Z_A)^2} + c.\Delta\delta \quad \textbf{(2.2)}$$

$$R_A^3(t) = \sqrt{(X^3(t) - X_A)^2 + (Y^3(t) - Y_A)^2 + (Z^3(t) - Z_A)^2} + c.\Delta\delta$$

$$R_A^4(t) = \sqrt{(X^4(t) - X_A)^2 + (Y^4(t) - Y_A)^2 + (Z^4(t) - Z_A)^2} + c.\Delta\delta$$

Equation (2.2) calculates the range R of the receiver and satellites coordinates that is extracted from the navigation message. The satellites coordinates are (X, Y, Z) and user's coordinates are (X_A, Y_A, Z_A) with clock bias $(\Delta\delta)$. These parameters are used to solve the PVT(Position, Velocity, Time). Since the previous equation is used in the case of four satellites detection, we can perform the necessary last square adjustments if more than four satellites are detected[13,14].

2.4 Error sources in GNSS

In the satellite navigation systems, there are several errors that can affect the performance of these systems, the next section will explain these errors in detail:

1. **Satellite clock error:** is it mainly caused by the satellite oscillator not being synchronized to the GPS time and it is one of the main errors which affect the positioning accuracy**,** the clock error is broadcasted from the satellite in the navigation message with respect to a reference time and it is modeled by the polynomial coefficients for example in GPS:

$$\delta^2 = a_0 + a_1(t - t_0) + a_2(t - t_0)^2 \quad \textbf{(2.3)}$$

   Where t is the GPS time, t_0 is the reference epoch time a_0 is the clock offset, a_1 is the clock drift coefficient, and a_2 is the clock drift rate coefficient[13, 15].

2. **Satellite orbital errors:** The receiver calculates a set of parameters within the navigation message that is called ephemeris data, which is constantly monitored and used to predict the satellite's movement in the control segment then the data is uploaded back to the satellites. Satellites transmit updated ephemeris data every 2 hours. recent prediction improves the clock data and ephemeris parameters, unfortunately over time accumulation of error is expected, this error is a root mean square (RMS) of about $2\,m$, the control segment can mitigate these errors by improving the prediction models [13–15].

3. **Ionospheric delay:** this delay occurs when the signal reaches the Ionospheric layer which is the upper layer of the atmosphere at an altitude of 1000 km above the earth, this layer contains various types of rapidly ionized gases that affect the signal transmit time. This delay is frequency dependent. Therefore, the best way to minimize this error is by transmitting a combination of two or multiple frequencies. Having multiple frequencies can give more advantages for ionosphere models to estimate the first and second-order effect of the ionosphere[14,15].
4. **Troposphere delay:** After the signal passes the Ionospheric layer it can reach the maximum height of 40km above sea level that is known as the troposphere, this part is composed of dry gases and water vapor. The troposphere consists of two different layers; the wet layer goes up to 10 km above sea level and causes 10% of delay; the dry layer is from 10km to 40km. unlike the Ionospheric delay, this delay is frequency independent, and it cannot be solved by using dual-frequency measurements but it can be mitigated by designing empirical models like Hopfield, and Saastamoninen models that consider different parameters; temperature, pressure, relative humidity, and mapping function[13–15].

   The previous atmospheric delays are also increased by the elevation angle which is the angle between the vertical plane (ground level) and a line pointing to the satellite as shown in Figure 2.3, the shortest distances between the receiver and the satellite are at zenith (elevation angle = 90°), therefore at low elevation angle the distance and atmospheric effects increases.

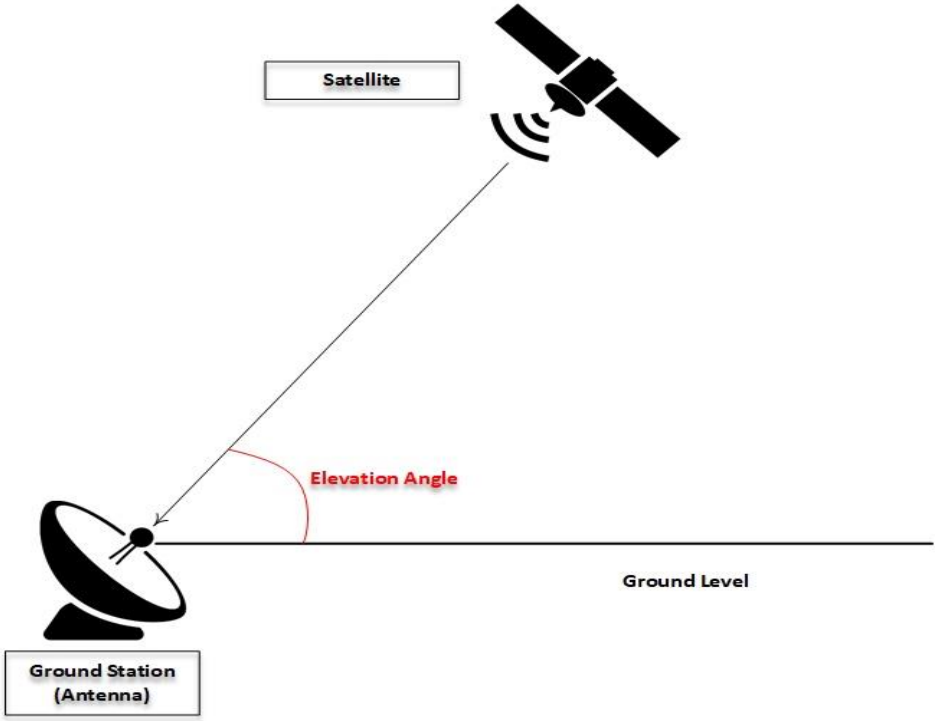

Figure 2.3 The elevation angle

5. **Receiver clock errors:** the receiver clocks are considered to be the cheapest clocks in the navigation system, which have low accuracy and can cause an offset between the receiver clock and GNSS reference time compared to other clocks as mentioned in section 2.3.1. This error can be solved in two different ways; the first way is using an external precise clock that has better performance, unfortunately, is it very expensive for the consumers; the second way is to consider this error as an additional unknown parameter in the position estimation process. For example, clock receiver clock bias ($\Delta\delta$) mentioned in section 2.3.2 [13–15].
6. **Multipath errors:** The satellite signal is expected to be received directly by the receiver. unfortunately, that's not always the case, the signal can be reflected on several objects (trees, cars, buildings ...) or the ground itself before reaching the receiver, this phenomenon is called multipath illustrated in Figure 2.4. This phenomenon distorts the original signal[14]. There are several ways to minimize this error; the first option is to place the receiver in a reflection-free location; however, this is not always a practical solution; the

second option is in the antenna and receiver design, designing an antenna that can mitigate the multipath effect and takes advantages of the signal polarization can almost eliminate the phenomenon[13,15], The “choke ring” antenna is one of the best-known antennas that mitigates multipath[16]

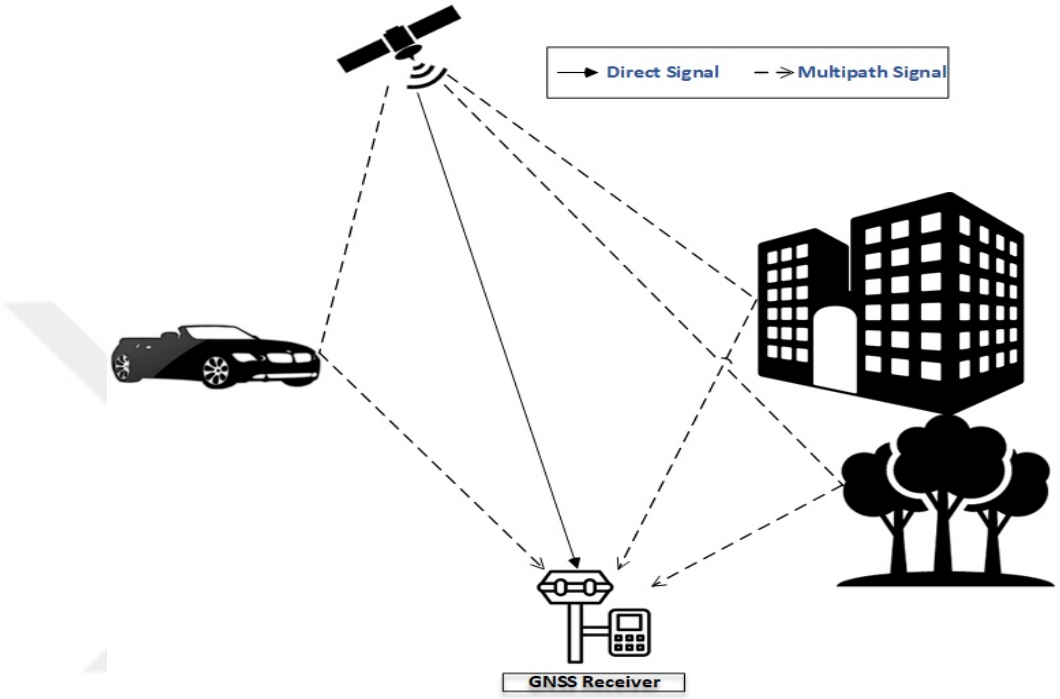

Figure 2.4 The multipath phenomenon

2.5 GNSS Signal Characteristics

the satellite constellations are responsible for constantly generating the radio navigation signals and transmitting them using single or couple frequencies in the L band. These signals consist of required parameters that allow the user to measure and extract the satellite to user receiver travel time and the satellite location. The fundamental GNSS signal consists of several components:

- Carrier wave.
- Ranging code.
- Navigation data.

The carrier wave is a simple sinusoidal wave set on a specific frequency that falls in the L band. All GNSS technologies use the carrier frequencies that are in the L band ranges.

The figure below shows the frequency bands within the L band for the Radionavigation Satellite Service (RNSS), there two bands of the L band: upper and lower L band. These bands allocated for Aeronautical Radio Navigation Service (ARNS) are very suitable for safety-of-life (SoL) applications. The upper L band (1559-1610 MHz) consists of the following GNSS signal; GPS L1, GLONASS G1, and Beidou B1 bands. The lower L band (1151- 1214 MHz) consists of; GPS L5, GLONASS G3, Galileo E5, and Beidou B2 bands. The rest of the GNSS signals: GPS L2, GLONASS G2, Galileo E6, and Beidou B3 signals are allocated within (1215-1350 MHz) bands because these bands are used for radio services (ground radars) which means they are more susceptible to interference then previous bands[9].

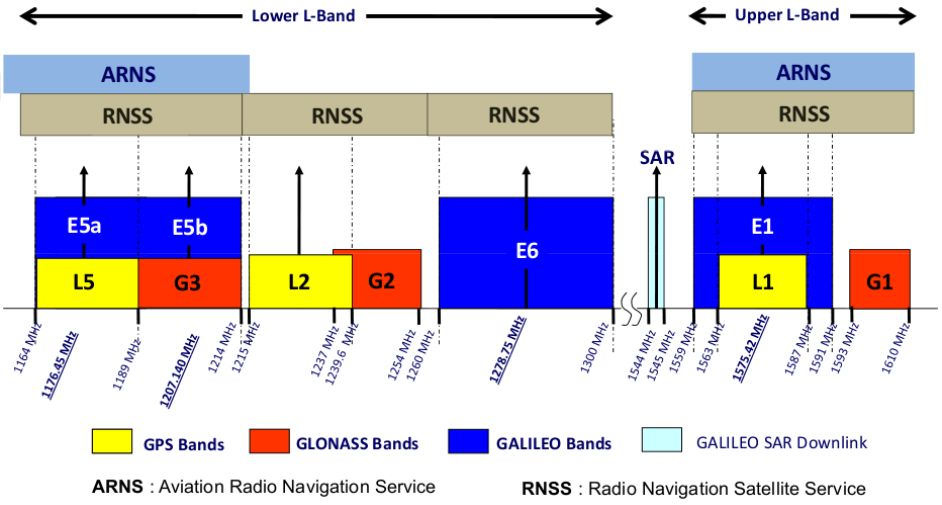

Figure 2.5 GNSS L-Band Frequencies

Ranging codes also known as Pseudorandom Noise (PRN) codes are sequences of 0s and 1s (zeroes and ones) which allow any receiver to determine exactly what satellite it is receiving from because each satellite within a GNSS constellation has a unique PRN code that it transmits as part of the C/A navigation message. The PRN codes

have a very low cross-correlation between them which mean that satellites will not interfere with each other.

The use of PRN codes is one of the important elements of Code Division Multiple Access (CDMA) technique to send different signals on the same carrier frequency but different PRN codes for specification, and the modulation method used is Binary Phase Shift Keying (BPSK)[9]. CDMA is used by all satellites in GNSS systems except for GLONASS which uses Frequency-Division Multiple Access (FDMA) technique to send a single with different carrier frequencies. Nevertheless, it requires higher complexity (and cost) regarding antenna and receiver design [9,17,18].

The navigation message is a binary-coded message that provides the receiver with all the essential information which are Ephemeris parameters to locate the satellites, the satellite Time parameters, Clock Corrections to detect the clock offset over time, the satellite operation status parameters, plus some other parameters. The message is transmitted at a quite slow data rate compared to previous signals, which is ranging from 50 bps to a few hundred bits per second. The user's Position, Velocity ,and Time (PVT) are calculated by the satellite after receiving the navigation message from the receiver [9,19].

2.5.1 GPS Signals

Legacy GPS signals are transmitted using two different carrier frequencies from the L band as shown in Figure 2.5, they are L1 and L2 bands their carrier frequencies are at $\mathrm{L1} = 1575.42\,\mathrm{MHz}$ and $\mathrm{L2} = 1227.60\,\mathrm{MHz}$ derived by the fundamental frequency $f_0 = 10.23\,MHz$ generated from a very stable clocks[20,21].

There are two main services provided by GPS:

- SPS: The Standard Positioning Service which is used by anyone and is free of charge, is Provided only by the L1 band frequency.
- PPS: The Precise Positioning Service is limited to only military and authorized users; it is provided by L1 and L2 bands frequencies.

GPS uses several PRN codes that are modulated with two carrier frequencies, these PRN codes are:

Coarse/Acquisition (C/A) code (Civilian code $C(t)$): is a sequence of 1023 chips that is repeated every 1 millisecond and transmitted at a chipping rate of 1.023Mchip/s, the total duration of each C/A code is 1 microsecond. This code is modulated only on L1 and used in the SPS service.

Precision code, $P(t)$: is a sequence of 6.187104x10^{12} chips that is repeated every 266 days (38 weeks) at a chipping rate of 10Mchip/s, The satellites are assigned a weekly portion of the code then modulated with the L1and L2 bands to be used in PPS.

Navigation message, $D(t)$: is a message that contains the time and position information of the satellite, and it is modulated with (C/A) and $P(t)$ codes at a 50bit/s as shown below:

$$s_{L1}(t) = a_P P_i(t) D_i(t)\, sin(\omega_1 t + \varphi_{L1}) + a_C C_i(t) D_i(t)\, cos(\omega_1 t + \varphi_{L1}) \quad \textbf{(2.4)}$$

$$s_{L2}(t) = b_P P_i(t) D_i(t)\, sin(\omega_2 t + \varphi_{L2}) \quad \textbf{(2.5)}$$

the i stands for i-th satellite.

In Figure 2.6 shows the legacy GPS satellite signal generation structure.

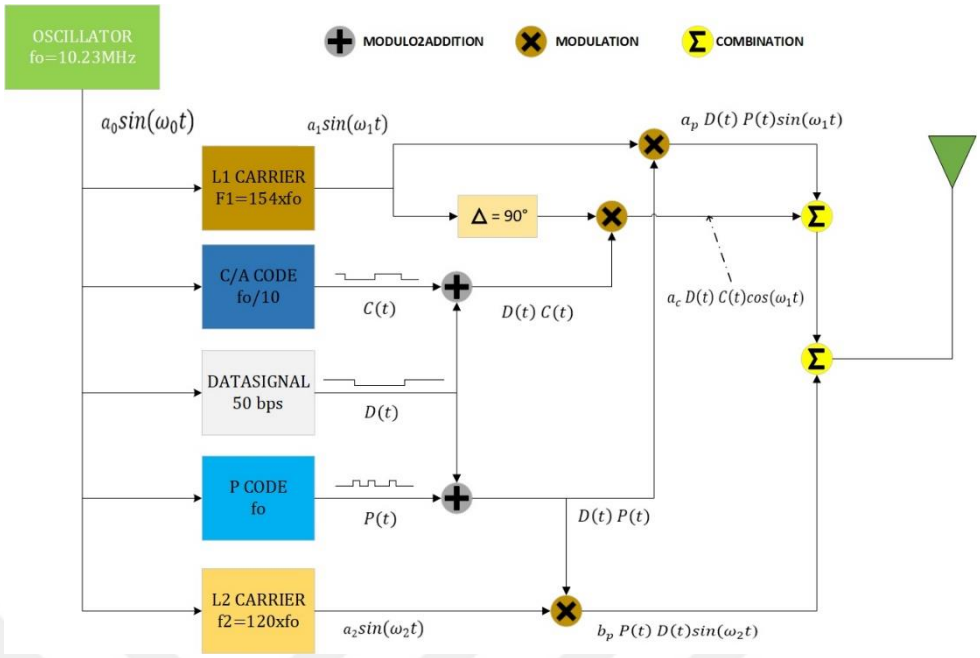

Figure 2.6 Legacy GPS satellite signal generation[9]

Table 2.1 Legacy GPS satellite signal[9]

Atomic clock frequency	$\boldsymbol{f_0 = 10.23\ MHz}$
Frequency L1 Wavelength L1	$\boldsymbol{154 \times f_0}$ 1575.42 MHz 19.03 cm
Frequency L2 Wavelength L2	$\boldsymbol{120 \times f_0}$ 1227.600 MHz 24.42 cm
P code frequency (chipping rate) P code wavelength P code period	$\boldsymbol{f_0 = 10.23\ MHz}$ **(Mchip/s)** 29.31 m 266 day, 7 days per satellite
C/A code frequency (chipping rate) C/A code wavelength C/A code period	$\boldsymbol{f_0/10 = 1.023\ MHz}$ 293.1 m 1 ms
Navigation message frequency Frame length Total message length	50 bps 30 s 12.5 min

2.5.2 Modernized GPS Signals

There are several GPS signals that modernized with their own new ranging PRN codes, for example, extra Link GPS L5, and the new civilian signals L2C, L5C, and L1C, plus the M military code[9].

Modernizing the GPS signals started with the launching of the first satellite in 2005 that supports L2C signals for civilian, commercial use and the modernized military signal (M-code) that is strictly limited for military use[22].

The L2C is a new civilian signal that is introduced in 2004, then started broadcasting in April 2014 on the same carrier frequency as the L2 band. This new signal contains 2 different PRN codes that are BPSK modulated to provide ranging information; the civil moderate code (L2CM) which is 10,230 chips long code that is repeated every 20 milliseconds at a chipping rate of 511.5 kchip/s, The second PRN code is civil long length code (L2CL) that is 767,250 chips long with a chipping rate 511.5 kchip/s and repeats every 1.5 milliseconds[22]. The precious codes are not exclusively used for the L2 band, they are used in the L1 band to produce another civil called L1C[23].

Military code signal (M-code) is a new way to encrypt military signals, and it is intended to eventually replace the precision code $\boldsymbol{P(t)}$ because of its ability to improve the ani-jamming and provide secure access to military signals. Mainly it is modulated at L1 and L2 center frequencies using Binary Offset Carrier Modulation (BOC) for more detail check [24], fortunately, M-code does not interfere with precision $\boldsymbol{P(t)}$ and $\boldsymbol{C/A}$ codes because it is designed to concentrate most of its energy is on the edges of the signal[22].

The last modernized GPS signal is the additional link (L5). It is transmitted at a carrier frequency ($\boldsymbol{L5 = 1176.45\,MHz}$) with a wider bandwidth that is completely reserved for aviation safety services. The L5 consist of two different signal PRN codes; In-phase code (I5-code) and quadrature-phase code (Q5-code) both are BPSK modulated 10,230 chips sequence broadcasted with a chipping rate of 10.23 MHz,

that is repeated every 1 millisecond. The I5 consists of data and 10-bit ranging code, and The Q5 consist of only 20-bit ranging code[9,22,23].

Table 2.2 Current and new GPS navigation signals. All civil signals are provided free of charge to all users worldwide (Open Services)[9]

Link	Carrier freq. (MHz)	PRN code	Signal Strength (dBW)	Modulation Type	Chipping rate (Mchip/s)	Data rate (bps)	service
L1	1575.420	C/A	−158.5	BPSK	1.023	50	Civil
		P	-	BPSK	10.23	50	Military
		M	-	BOC	5.115	N/A	Military
		L1C-I data	−157	MBOC	1.023	50	Civil
		L1C-Q data				-	
L2	1227.600	P	-	BPSK	10.23	50	Military
		L2CM L2CL	−160	BPSK	1.023	25	Civil
						-	
		M	-	BOC		N/A	Military
L5	1176.450	I5 data	−154.9	BPSK	10.23	50	Civil
		Q5 pilot				-	

CHAPTER 3

RECEIVERS ARCHITECTURES

3.1 Introduction

The first advent of the wireless communication system was the Marconi's demonstrated viable radio system in 1895, The early equipment was crude and very insensitive; now the receivers are very sensitive and offer wide variety of applications. The high demand for radio frequency transceivers has increased rapidly due to the wireless communication evolution in the world. These demands require a low cost, low power and small size modern receivers, therefore different types of receivers have been proposed, such as super heterodyne receivers, heterodyne receivers, Low-IF receivers, Zero-IF/ Low-IF Multi-standard receivers, Wideband IF Double conversion receivers, Digital-IF receivers, and Direct Digitization receivers (DRFS). Each architecture is being used based on their requirements because each architecture is different in features. This chapter will explore in brief the main features of different architectures.

3.2 Super Heterodyne Receivers

The super-heterodyne receiver architecture was invented in 1918. It has been the most commonly used architecture till today and this is due to its good selectivity, sensitivity as well as image rejection. Even though, some modifications have been made compared to the pilot architecture. Needful to note is that most receiver designs have been established on the super-heterodyne principle [25]. This receiver configuration essentially translates an input RF signal to a lower-frequency known as intermediate-frequency (IF) signal. Figure 3.1 shows the architecture of a super-heterodyne receiver.

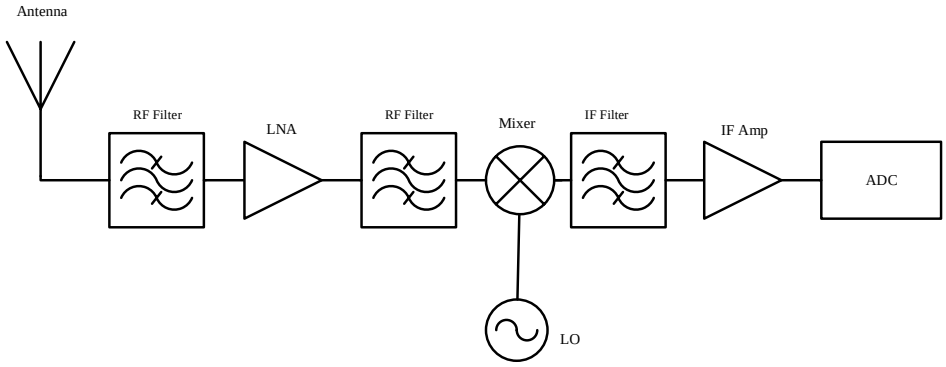

Figure 3.1 The traditional super-heterodyne receiver

Considering Figure 3.1, a received signal enrolls into a band-pass filter (often referred to as a pre-select filter) that winnows out the out-of-band signals and thereafter to the low-noise amplifier (LNA) for amplitude amplification. The LNA is an exceedingly important component, as the overall noise figure of the receiver is extremely dependent on its noise figure. Some other band-pass filter that is commonly referred to as the image-reject filter, postdates the LNA. The primary role of this filter is to pass up the undesired image frequency band.

Thenceforth, the RF signal gets into a mixer that converts it to a lower-frequency signal which is normally known as the Intermediate Frequency (IF) signal. This is done by mixing it with the LO signal. The IF is the difference between the input RF signal frequency and the LO signal frequency.

After down converting the signal to IF it is subjected to band-pass filtering then to an IF amplifier that provides it with the necessary gain. The amplified IF signal is thereby intromitted to the ADC for demodulation and further signal processing.

However dual-conversion heterodyne receivers are oftentimes used due to various fundamental advantages (hence the common term “super-heterodyne”). This approach is more suitable for higher-frequency applications like military and radar. A dual-conversion heterodyne receiver is shown below as illustrated in [25].

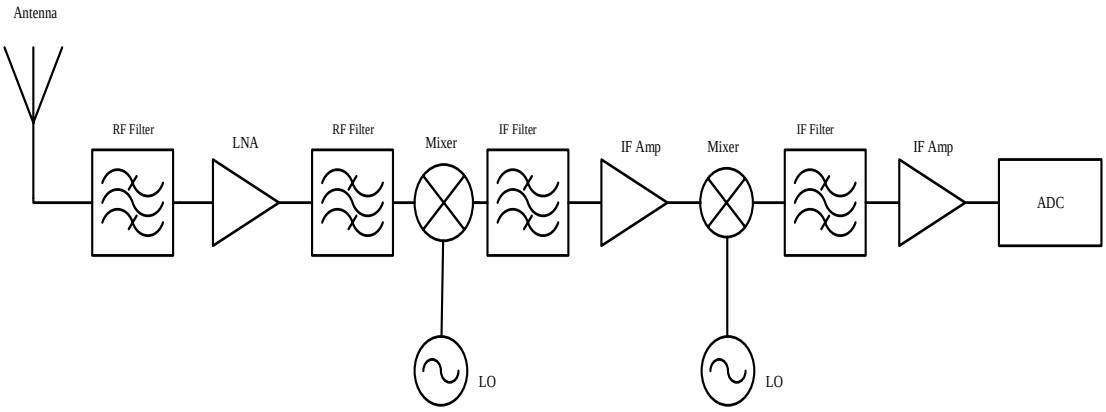

Figure 3.2 The dual conversion super-heterodyne receiver

In dual-conversion receivers there are two mixers and two local-oscillators (LOs) thereby performing conversion at two stages. The first mixer converts the input RF signal to a lower frequency (first IF) by mixing it with the first LO signal. Then the second mixer converts the first IF signal to a much lower frequency, which is the second-IF frequency by mixing it with the second LO signal [25].

The advantage of dual-conversion receivers is the fact that they have a higher first-IF frequency which gives them the ability to attain salutary image rejection. Moreover, such dual-conversion receivers are also capable of achieving good selectivity owing to the fact that they have a lower second-IF. Hence, dual-conversion (super-heterodyne) receivers are formidable candidates when it comes to salutary image rejection and excellent selectivity.

However, the main challenge that presents itself in these receivers is the image frequency band. It's a noteworthy fact that an elementary multiplier does not uphold the polarity of the difference between its two input signals [26]. For example, let's assume two signals.

$$x_1(t) = \cos w_1 t \quad \textbf{(3.1)}$$

$$x_2(t) = \cos w_2 t \quad \textbf{(3.2)}$$

The low pass filtered product of the above two signals will be $\cos(w_1 - w_2)t$ which will not be different from $\cos(w_2 - w_1)t$. Thus, the bands that are above and below the frequency of the LO symmetrically are down converted to the same frequency. Furthermore, when an input RF signal and an LO signal enrolls to a mixer, a low frequency (Intermediate Frequency) signal is generated at the output of the mixer. This Intermediate Frequency (IF) is the difference of the frequency of the input RF signals and the frequency of the LO signal. Nevertheless, another input RF signal with the same LO signal may get into the mixer and render the same IF signal. This other input RF signal is commonly referred to as the image frequency signal. It may be expressed as:

$$|f_{RF} - f_{LO}| = f_{IF} \quad \textbf{(3.3)}$$

$$|f_{IM} - f_{LO}| = f_{IF} \quad \textbf{(3.4)}$$

Where:

f_{RF} is the input RF signal frequency.

f_{LO} is the LO signal frequency.

f_{IF} is the of the IF output signal frequency.

f_{IM} is the image signal frequency.

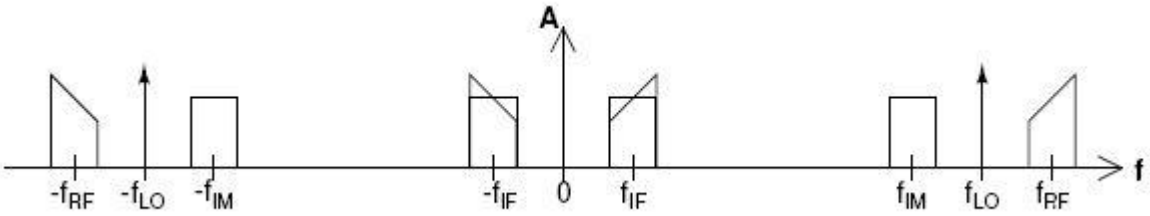

Figure 3.3 The image problem in super-heterodyne receivers

In order to inhibit these undesired image frequencies in a super-heterodyne receiver, it is a common and necessary practice to have a filter preceding the mixer. Even so, down-converting a signal with a very high-frequency to a low-frequency in barely one stage may be catastrophic to the receiver. This is because the image frequency band will certainly be very near to the input RF band. Hence, filtering these image frequencies thoroughly proves to be a significant challenge because of their propinquity to the real input RF frequencies [25].

However, a dual-conversion configuration can remediate this problem whereby it can make it distinctively possible to put a considerable space between the image frequency band and the real RF input frequency band. This increased spacing between the image frequency band and the input RF frequency band is because of the relatively higher first-IF. Down-converting the input RF frequency to a first-IF allows the image frequency band to be relatively further away compared to converting the input RF frequency directly to the lowest final IF.

Accordingly, filtering these image frequencies becomes easier however at an expense of adding more components which is costly and even, so the power needed to drive these added components tend to lead to relatively higher power consumption [27].

3.3 The Homodyne Receiver

This is also known as the zero-IF or direct conversion receiver. In this receiver architecture, the received RF signal is selected by a band-pass filter, amplified by a low noise amplifier LNA, and then it is down converted to DC directly by a mixer or they maybe two mixers that have a delay of 90º between them. Thereafter it is

converted to the digital domain by the ADC. Since in this kind of receiver the desired channel center frequency is translated to DC, which is 0 Hz, the negative part of the channel on the frequency axis becomes the image to the positive part and vice versa. Hence, there's need for complex signal processing to reconstruct the down-converted signal for the negative part of the channel not to be penned up in the positive part. Thus, two down-conversions are executed; for the in-phase component (I) and for the quadrature-phase component (Q). It should also be noted that a low pass filter (LPF) is used in the homodyne receiver. This LPF may be designed by on-chip active filters thereby obviating the use of external filters hence rendering a high level of integration. More so, if these filters may be programmable, multiple frequency bands may be used [28]. A homodyne receiver is shown in the Figure 3.4 as illustrated in [29].

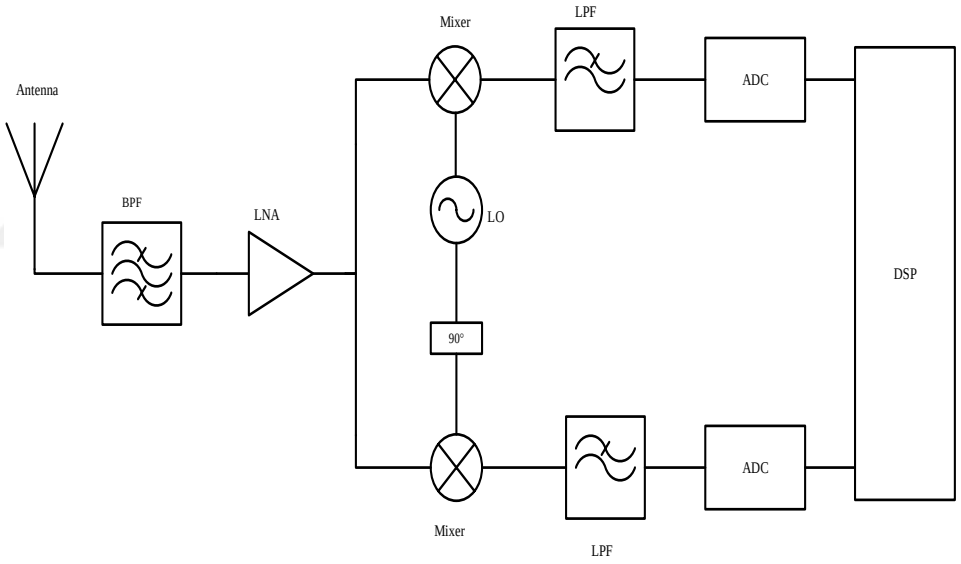

Figure 3.4 Homodyne receiver

The advantage of this architecture is that it has less analogue components compared to the super-heterodyne architecture and guarantees a high level of integration.

However, in spite of its simplicity in contrast to the super-heterodyne receiver, most components of the homodyne receiver are extremely complex to implement. Additionally, the direct conversion to DC may induce various problems which highly restricts the use of this receiver configuration instead of the super-heterodyne [30].

These problems include:

- Local oscillator (LO) leakage that's brought about by the non-ideal isolation between the mixer ports due to capacitive and substrate coupling as well as bond wire coupling if the LO is externally provided [26]. A similar effect may be caused by interferer leakage from the low noise amplifier (LNA) or the input of the mixer to the LO.
- I/Q mismatch because of the errors in I/Q modulation.
- Even/Odd-order distortion generated by the prevalent non-linear components which always lead to harmonics especially second-order intermodulation products that are always around DC.
- Flicker noise (1/f noise) which is basically a problem at low frequencies. And since now the signal is at DC, it is susceptible to this kind of noise.

3.4 The Low-IF Receiver

A somewhat similar receiver configuration to the zero-IF receiver is the low-IF receiver. In this receiver, the RF signal is down-converted to a low (non-zero) IF which can range from a few hundred kHz to a few MHz and this is achieved by quadrature RF down-conversion. This configuration attempts to aggregate the advantages of the super-heterodyne and zero-IF receivers. Like for the case of zero-IF receiver, the received RF signal goes through a channel-selection filter and then through LNA for amplification. Thereafter, the signal is down converted to a low IF. An image suppression block is used to cancel the negative effects of the frequency image. Finally, the signal is converted to digital domain by the ADC. Nonetheless in some low-IF receiver architectures, the image suppression block is also carried over to the digital domain. The Figure 3.5 below shows a low IF receiver as illustrated in [30].

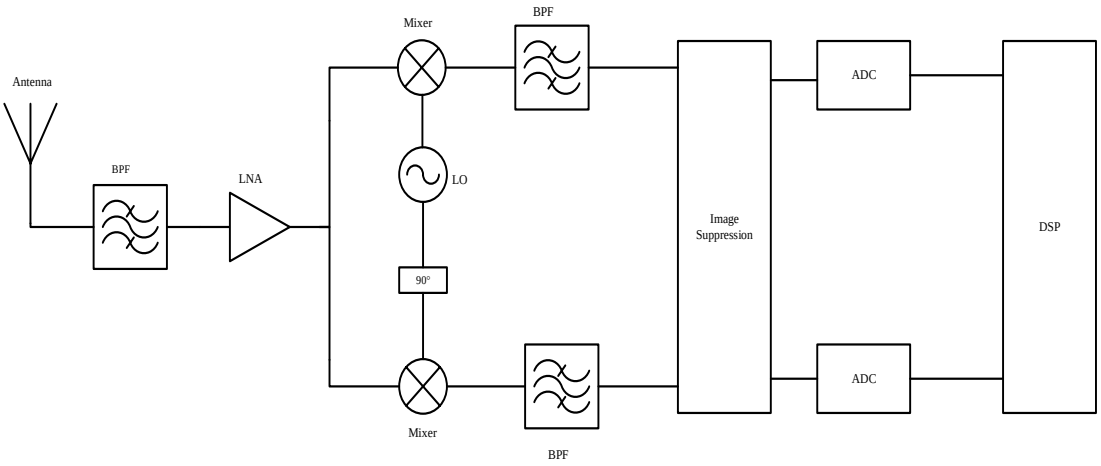

Figure 3.5 The low- IF receiver

The advantage of this receiver architecture is that it allows for a considerably high level of integration and in addition to that it is not subjected to DC problems owing to the fact that the wanted signal is not posited around DC.

However, the challenge with this receiver architecture is that it suffers from I/Q mismatch and image frequency problems to even a greater extent than what is incurred in both the super-heterodyne and homodyne receivers. More so, the power consumption of the ADC is relatively increased because of the higher conversion rate required.

3.5 The Direct Radio Frequency Sampling (DRFS) Receiver

Direct Radio Frequency Sampling is the technique of digitizing the input signal directly at RF with an ADC, without first down-converting it to a baseband frequency (Zero IF) or a lower IF [31]. In this technology a DRFS ADC replaces the receiver's analog components such as mixers, local oscillators, intermediate frequency filters and amplifiers as shown in the Figure 3.6 below which is illustrated in [32], thereby melting off the cost of materials, size, power consumption, design time and weight, whilst enhancing the flexibility and software programmability of the entire system.

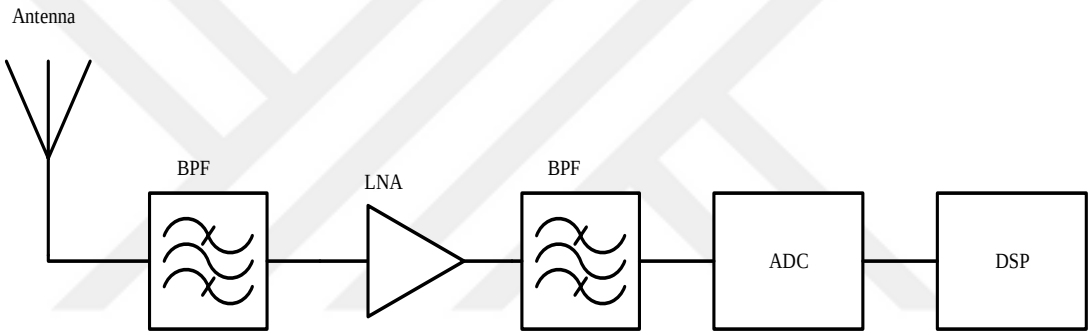

Figure 3.6 The direct radio frequency sampling receiver

Direct radio frequency sampling (DRFS) receiver architecture, with a Nyquist ADC is increasingly proving to be the preferred practical alternative to the traditional super-heterodyne receiver architecture. In traditional receivers like the super-heterodyne, designers usually choose the analog-to-digital converter (ADC) depending on primary specifications like the dynamic range and the signal to noise ratio (SNR). However, for the case of a DRFS receiver, the designers' special emphasis is rather on the effect of the ADC on the receiver noise figure [33].

Nonetheless, it is still doubted whether the direct radio frequency sampling configuration will ever contend in power-restricted applications, except when the application requires to enamor a relatively big portion of the Nyquist bandwidth [34].

It’s also noteworthy that one of the primary concerns of a DRFS receiver architecture is its operation with high gain for which the traditional super-heterodyne and homodyne receivers have been optimized for a long time [33].

- A DRFS receiver provides significant flexibility when it comes to frequency planning. This is undoubtedly an indispensable requirement in wireless communication because of the innumerable possible interferers [35].
- Since a DRFS receiver gets rid of several analog components like the mixer and the LO, this typically means better noise figure as well as lower cost. More so, the LO spur and image frequency issues are all trounced.

However, for optimum performance of DRFS receivers there are some challenges that need to be curbed. Nonetheless, these challenges depend on the application whereby some may be more critical. Below is an clarification of these challenges as they were thoroughly exposited in [32];

1. Receiver sensitivity: this is one of the primary receiver performance specifications. It refers to the weakest signal that a receiver can detect and process. It should be noted that it is impossible for a weaker signal to be successfully demodulated if the noise in the demodulated bandwidth is relatively more salient than the received signal.
2. Radio performance in presence of in-band interferer; it is not uncommon for interferers to get ascribed in the receiver’s filter passband henceforth it is required to ascertain how well the receiver can substantially demodulate weaker signals whilst the presence of in-band blockers. It is known that the automatic gain control (AGC) controls the blocker power level below the input full scale of the ADC to avert saturation. Nevertheless, the blocker harmonics that are brought forth in the ADC during the sampling may fall onto the weak desired signal thereby contracting the receiver’s demodulation ability.
3. Radio performance in presence of out-of-band blockers; regardless of the configuration, the input of the ADC must be concealed from prominent out-of-band blockers because this may alias the in-band to outstrip the ADC full

scale and lead to receiver saturation or lead to harmonics that may overlap the in-band desired signal. It should be remarked that the design for DRFS receiver filters is somewhat unstrained especially when frequency planning is implemented. There are no LO spurs or image frequencies issues however, interleaving spurs for out-of-band blockers and low-order harmonics need to be carefully dealt with.

4. Sampling clock performance: in a DRFS receiver, the sampling clock of the ADC is like the LO of the super-heterodyne receiver. The requirements of the clock phase noise always depend on the application. Hence, it is good to always define the phase noise at offset frequencies of a given application instead of integrating it across the entire Nyquist zone for a given jitter number. Moreover, in this state of affairs, the clock is a radio frequency signal and is subject to more challenges like attenuation. Thus, there is need for considerably high clock amplitudes for low noise floor and elusive skew management especially in multi-channel systems [31].

3.6 Software Defined Radio (SDR)

The riotous egression of wireless communication standards revs up the indispensability of multimode radio receivers and even so, low power consumption, low cost and high flexibility are all primal issues. One way to realize flexible and multimode configurations is by using Software-Defined Radio (SDRs) [36], a term that was coined in 1991 by Joe Mitola to relate to reconfigurable radios [29], [37]. SDR can be defined as a radio in which some or all the physical layer functions are software defined. Otherwise stated, the software is used to ascertain the radio specifications and what it does. If the software within the radio is changed, its performance and functions may change.

Another definition that may embrace the central meaning of SDR is that it has a generic hardware platform on which the software runs to provide functions such as modulation and demodulation, filtering, as well as frequency selection and frequency hopping. To execute those functionalities, the software defined radio technology uses software modules that operate on a generic hardware platform having digital signal

processors as well as general purpose processors to implement the radio functions of transmitting and receiving signals. Implementing the ideal software defined radio would require digitizing the signal as early as possible at the RF chain like in DRFS receivers shown in Figure 3.7 which helps in handling a broad range of frequencies and allow flexibility in the digital domain.

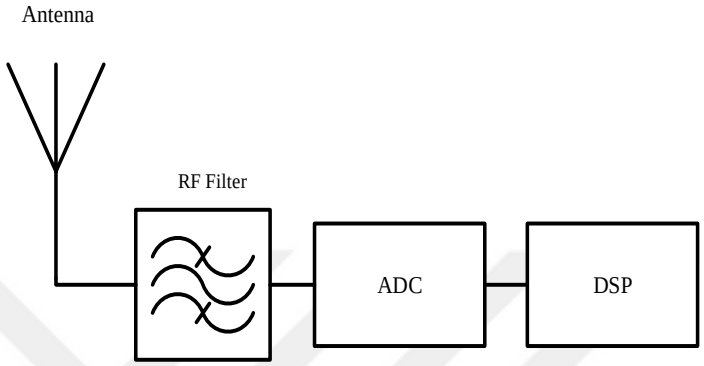

Figure 3.7 An ideal software defined radio receiver

Conceptually, the above configuration is provided with an ADC of good sensitivity and sampling rate as well as a dynamic range. However, it imposes strict requirements on the ADC performance and would result into extraneous power dissipation.

In general, SDR may be regarded as the expansion of digital signal processing towards the antenna which necessitates improvements in the input bandwidth and the dynamic range of the ADC at a cost of increased power consumption. This means the need to carefully choose the appropriate ADC since the increased bandwidth justifies that more signals (wanted and unwanted) need to be processed because they have not been thoroughly filtered out earlier in the receiver chain.

3.6.1 Advantages of Software Defined Radios

Software Defined Radios have got innumerable advantages, and this justifies the fact that they are being used in a great deal of applications such as military, radar, satellite modems and cellular technology. Below is an elucidation of some of those advantages as explained in [13]:

- A software-defined radio tolerates changing the identity of the radio in real-time, which reasonably guarantees a desired Quality of Service.
- The flexibility in the architecture helps service providers to upgrade the infrastructure and have their new services marketed easily and quickly.
- The architecture of software-defined radios gives systems new capabilities which can be easily implemented by software. For example, sometimes typical upgrades may need software-enabled power control, encryption, interference rejection technics, voice recognition, and advanced error recovery schemes.
- Since software-defined radios typically have less analog components, this translates into a reduction in cost of materials, size, power consumption, design time and weight.

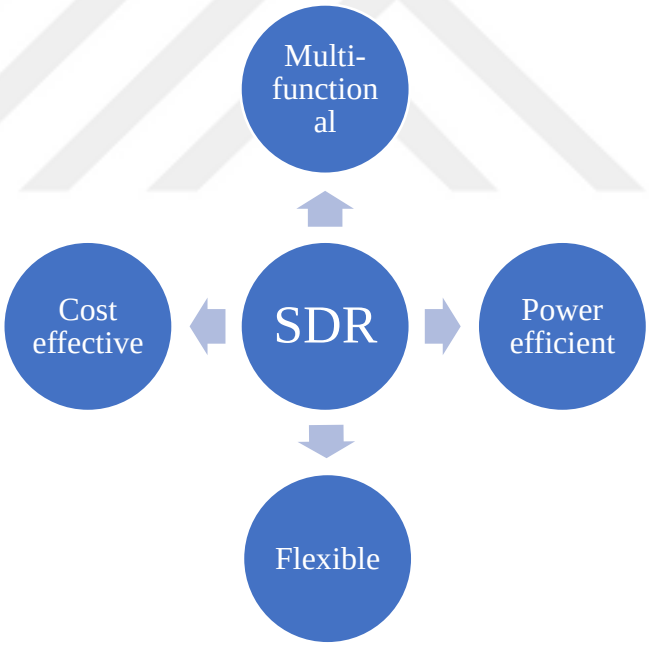

Figure 3.8 SDR advantages

In summary:

However, it should be noted that there are some limitations to the universal application of SDRs which include but not limited to:

- The indispensable need for convoluted interfaces to signals in digital domain.
- Complexity in writing the software for certain systems.
- Designers' deficiency in understanding the primary requirements.

In a nutshell, the software-defined radio typifies a substantial change in the design epitome for communication radios whereby a great part of the functionalities is implemented in digital domain through flexible and programmable digital signal processors, thereby giving a radio the potential to alter its parameters for new capabilities and features. More so, a software-defined radio subdues the RF content and other analog components of a radio thereby enhancing the receiver flexibility. Today, the wireless communication systems developers and service providers are so much interested in SDRs.

3.7 Receivers Design Considerations

A receiver performance is limited by four main factors: noise, nonlinearities, circuit imbalance and components quality factor. These factors are mainly used to define the parameters of a radio receiver, which are noise figure, sensitivity, selectivity, Dynamic Range, baseband performance and frequency range, we will expand more on Some of them in the following sections [38]:

3.7.1 Noise Figure

Noise figure is the measurement of the signal to noise ratio in decibels (dB) between the input and output of system. SNR will always suffer a reduction because in real systems generally the output noise power will be amplified the same as the signal and the component under consideration will add its self-generated noise to the output too. The noise figure F equation is:

$$F = \frac{SNR_i}{SNR_o} = \frac{S_i/N_i}{S_o/N_o} \geq 1 \qquad \textbf{(3.5)}$$

S_i and N_i are the input signal and noise power, and S_o and N_o are the output and noise power, The input noise is considered as a thermal noise produced when power

from a component or source is absorbed by a matched load at standard noise temperature $T_0 = 290k$,The input noise N_i is defined as:

$$\mathrm{N}i = K\mathrm{T}0B \quad \textbf{(3.6)}$$

Where K is the Boltzmann constant and B is the equivalent noise bandwidth, noise figure NF in dB is obtained from equation below:

$$NF(dB) = 10log\ (F) \quad \textbf{(3.7)}$$

For cascaded systems with an m stages the total F can be obtained using Friis Equation below [39]:

$$F_{Total} = F_1 + \frac{F_2 - 1}{G_1} + \frac{F_3 - 1}{G_1 G_2} + \cdots + \frac{F_m - 1}{G_1 \ldots G_{(m-1)}} \quad \textbf{(3.8)}$$

Where F_m is the noise figure and G_m is the power gain (linear) of stage m calculated with respect to the input impedance. As can be seen in equation (3.8), the first amplifier in a chain usually has the most significant effect on the total noise figure. Therefore it is preferable that the first stage should have low noise and gain, that's why the first amplifier is mostly picked to be a low noise amplifier [10,38].

3.7.2 Sensitivity

Receiver sensitivity is the measure of the minimum signal strength that a receiver can cope up with at an acceptable signal-to-noise ratio to maintain service quality. One possible issue that we might face in direct multi-GNSS sampling receiver that the output desired signal interferes with unwanted noise at the same frequency band, in consequence affect the sensitivity. There is a conventional way to calculate the sensitivity using the noise figure. If the receiver input has only one desired signal, the input noise plus the receiver internally generated noise is what is responsible for the sensitivity value[38].

The calculations to extract the sensitivity equation start the by expanding F:

$$F = \frac{SNR_i}{SNR_o} = \frac{P_i/N_i}{SNR_o} \quad \textbf{(3.9)}$$

We can rearrange to find the input signal power P_i from pervious equation:

$$P_i = N_i \cdot F \cdot SNR_o \quad \textbf{(3.10)}$$

by adding the input noise power N_i that is given by:

$$N_i = KT_0B \quad \textbf{(3.11)}$$

by substituting **(3.10)** and **(3.11)** and obtain $NF(dB)$ from equation **(3.7)** we get:

$$P_i[dBm] = 10\log(KT_0B) + NF(dB) + SNR_o[dB] \quad \textbf{(3.12)}$$

$10\log(KT_0B) = 174dBm/Hz$ therefore, it can be replaced in **(3.12**) to give us:

$$Pi[dBm] = 174dBm/Hz + NF(dB) + SNR_o[dB] \quad \textbf{(3.13)}$$

Derived from the noise figure equation we can determine the receiver parameters trade-offs for any input signal level using sensitivity equation (3.13).

3.7.3 Selectivity

In modern receiver design selectivity is the ability to detect and demodulate the desired signal of interest from the unwanted interfering signals. The non-linear behaviors of active components generate an overload, modulation distortion, spurious signals and spurious responses, these effects are minimized in the direct multi-GNSS sampling receiver by adding filters which increases the selectivity.

Filters are very crucial elements in the receiver performance due to their contribution to both selectivity and sensitivity issues [40].

3.7.4 Dynamic Range

Dynamic range has two different definitions (DR). It is defined as the maximum tolerable desired signal power divided by the minimum tolerable desired signal as shown in Figure 3.9**.** This concept is applied in several applications mostly in analog devices like amplifier and ADC.

The second definition of the dynamic range is called Spurious-free dynamic range (SFDR) is the ratio between Desired signal of interest to the strongest spurious signal in the output. As explained in Figure 3.9 Sensitivity of receiver is defined as the lower end of the dynamic range and the upper end is defined as a single maximum input level that receiver can handle without effecting the quality of the signal [10,38].

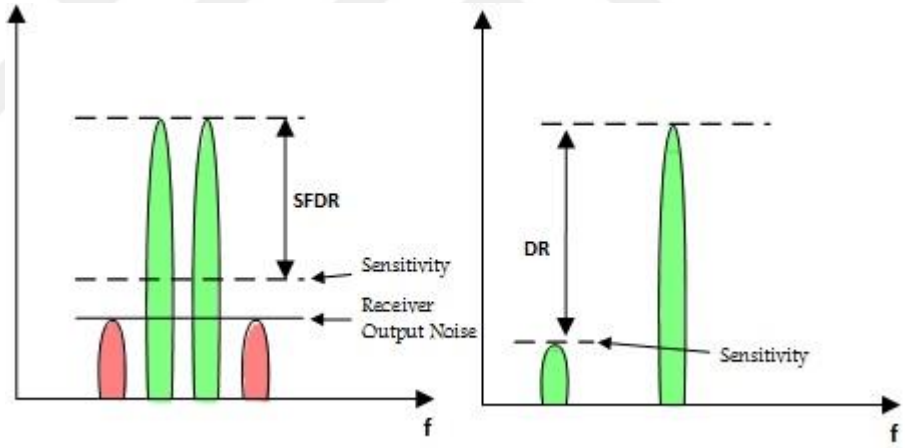

Figure 3.9 Dynamic range and SFDR illustration[38]

3.8 Spectrum Analysis Of A Multi-GNSS Direct Radio Frequency Front-End

The analysis in this section can be done by considering multiple signals in different bands that are received by the antenna and amplified by the LNA. The received signal model can be expressed as:

$$y(t) = \sum_{j=1}^{M} A_j(t) \cos\left[2\pi f_{cj} t + \varphi_j\right] + n(t). \quad \textbf{(3.14)}$$

In the above equation, M signals from multiple bands are considered (received) with nominal carrier frequencies f_{cj} for j $= 1, \dots, \dots$, M with an envelope amplitude of $A_j(t)$, phase φ_j and bandwidth B_j ,while the term $n(t)$ represents noise and interfering signals.

Viewing the spectrum of the considered signals in frequency domain provides an insightfulness, and that can be done by Fourier transformation to transform the time-domain signal to frequency domain.

$$y(w) = \int_{-\infty}^{\infty} y(t) \times e^{-iwt}\, dt \quad \textbf{(3.15)}$$

Applying the Fourier transform on a single band model, $M = 1$, the spectrum we can be expressed as:

$$y(w) = [e^{j\,\varphi_j} A_j(w - w_c) + e^{-j\,\varphi_j} A_j(w + w_c)\,]/2 + n(w) \quad \textbf{(3.16)}$$

As can be seen from the Direct RF receiver diagram in Figure 1.3 there are M bandpass filters that should leave $A_j(t)$ and φ_j largely unaffected, while attenuating most of the out-of-band noise and interference contained in $n(t)$. That is mainly because the M signals are considered to be band-limited or bandpass signals. After filtering, the signal is sampled with a specific sampling frequency w_s of the ADC which can be modeled, in the frequency domain, as[41]:

$$y(w) = \frac{1}{T_s} \sum_{k=-\infty}^{\infty} y(w - k w_s) \quad \textbf{(3.17)}$$

The value of w_s is very crucial, as will be explained in section 3.9, in DRFS receivers for handling signals appropriately. The value of w_s can be calculated based on the bands of the signals considered by the DRFS receiver. This calculation can be very complicated, but in this research, we are introducing a methodology that minimize the complexity which as explained in detail in section 3.9.

In case of considering (receiving) multiple band-pass signals, equation (3.17) can be generalized as:

$$y(w) = \frac{\pi}{T_s} \sum_{k=-\infty}^{\infty} e^{j\varphi_j} A_j(w - w_c - kw_s) + e^{-j\varphi_j} A_j(w + w_c - kw_s) + OONF(w - kw_s) + n(w) \quad \textbf{(3.18)}$$

$OONF(w - kw_s)$ stand for (sampled out of band noise), it is considered as the out of band noise that is sampled and not filtered by the bandpass filter, and it also occur due to noise folding, the output of the ADC can be modeled in time domain as:

$$y(t) = \sum_{j=1}^{M} A_j(t_l) \cos\left[2\pi f_{if\,j} t_l + \varphi_j(t_l)\right] + V_j. \quad \textbf{(3.19)}$$

Where equation (3.19) refers to the sample time $t_l = l\Delta t_s = l/f_s$ with sample period Δt_s and sampling frequency $f_s = 1/\Delta t_s$. The sequence $v_0, v_1, v_2, \dots, v_l, \dots$ is the discrete-time noise. $f_{if\,j}$ is the intermediate frequency which is the down converted center carrier frequency f_{cj} of the band-pass signal after sampling (as explained in 3.9). In the next part we will explain in details the effects of the ADC on the sampled signal discrete-time noise V_j [42,43].

3.9 Frequency Planning Of Direct RF Sampling Receivers

Direct RF sampling is a radio receiver technique in which the RF signal of interest is directly sampled which results in aliasing the signal spectrum to lower IF value in the

basic Nyquist band (as well as to other higher bands) without the need for a mixer as explained in detail in section 3.5. Sampling an RF signal centered at a frequency f_c directly using the ADC will require us to follow the Nyquist theorem which states that the sampling frequency f_s of the ADC should be slightly higher than twice the highest frequency$f_s \geq 2f_c$) (, to make the sampled RF signal aliasing free in the baseband f_{IF} which falls in the Nyquist zone interval $(0, \frac{f_s}{2})$. However, applying the Nyquist theorem can be impractical due to the high sampling rate requirement in our case[44], for example, GPS L1 at $f_c = 1575.2\text{Mhz}$ needs a sampling frequency of at least $f_s = 3150.84$ Mhz. This can be demanding on the ADC, thus limiting the full potential of our architecture. The best acceptable solution for this impracticality is to utilize the concept of bandpass sampling[41], [44–46].

Bandpass theorem states that when the continuous bandpass signal of interest is sampled with a sampling frequency that is more than twice the signal's bandwidth $f_s \geq 2BW$ allows sampling at a much lower frequency than its original carrier frequency since the sampling requirements are based on the information bandwidth of the signal rather than the carrier frequency[46]. A high-level frequency-domain depiction of this process is based on the direct sampling front end from Figure 1.2 and it starts by using the appropriate bandpass pre-filter so that the input signal to the ADC can be a clean bandpass signal which helps reduce the memory requirement necessary to capture a given time interval of a continuous signal [46] or the computational resources needed for directly processing it. Hence, we can exploit the bandpass sampling technique to work with the bandpass filtered single from multiple bands using a single front-end.

When it comes to choosing the sampling frequencies f_s, a set of equations are used to represent the constraints on f_s. Those constrains include, [47]:

- The sampling frequency should be at least twice the bandwidth of the signal $f_s \geq 2BW$.
- Choosing an f_s to avoid any overlap between aliased bands from the negative and positive frequency spectrum and the baseband Nyquist zone lower end at 0 or upper end at $\frac{f_s}{2}$.

- f_s is properly selected to minimize the noise folding and its effects as explained in section 3.9.3.

While considering these constraints, two algorithms are proposed to find the valid sampling frequencies f_s for two different cases:

Case1: Is in the existence of single band-limited signal, like GNSS signal; GPS L1 band where the algorithm is explained in details section 3.9.1.

Case2: Is in the case of multi band-limited signals like, GPS L1, L2 and L5 and it is explained in detail in section 3.9.2.

To start extracting the equations used in the algorithms mentioned previously, we need to consider a spectrum of a continuous bandpass signal with bandwidth BW, located between the positive lower frequency f_l Hz and higher frequency f_h Hz with a center frequency f_c. The signal bandwidth BW is less than $f_h - f_l$, and the positive frequency band can be expressed as the interval (f_l, f_h). The negative frequency band can be expressed as the interval $(-f_l, -f_h)$ with a center frequency of $-f_c$ as shown in Figure 3.10(a). furthermore, we need to consider an arbitrary positive integer N that equals to the integer part of $\frac{f_c}{f_s}$ and ensures $f_s \geq 2BW$, N can be either even or odd. If N is Even, we denote the sampling frequency as f_{s1}. In this case, the sampled positive frequency spectrum exists in +ve baseband Nyquist zone as shown in Figure 3.10 (b), whereas if $N\ is\ Odd$, we denote the sampling frequency as f_{s2}. In this case, the sampled negative frequency spectrum in -ve baseband Nyquist zone as shown in Figure 3.10 (c).

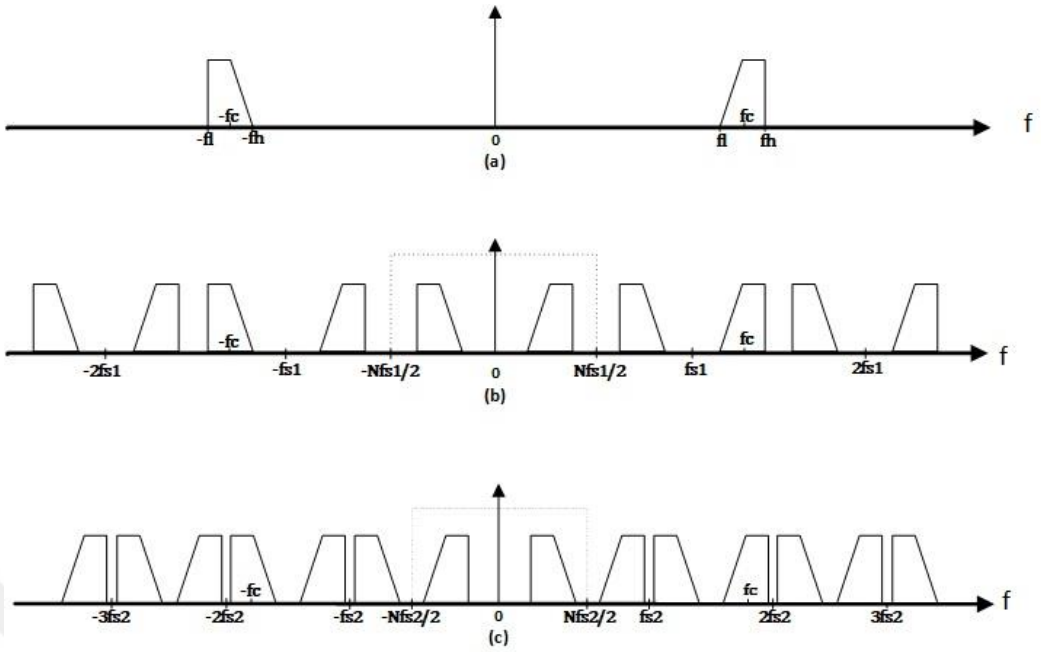

Figure 3.10(a) the original, (b) the sampled signal by sampling frequency fs1 (N=Odd) and (c) the sampled signal by sampling frequency fs2 (N=Even)

The spectrum of the sampled signal can be obtained by replicating the spectrum of the original signal at Nf_s around f_c. Accordingly, the spectrum of the original signal must not straddle $N\frac{f_s}{2}$ for any integer N, otherwise the sampled signal would be aliased [19], therefore the entire positive spectrum of the original signal must lie in the frequency range $(N\frac{f_s}{2}, (N+1)\,f_s)$. The choice of N has a big effect on the noise folding that is explained in section 3.9.3 the smaller the N value the less folding will accrue for example in our case $GPS\,L1 = 1575.42MHz$ is sampled with $f_s = 300\text{MHz}$ which means that signal is going to be folded 5 times. Consequently, using smaller sampling frequency will generate more noise folds.

we can develop a set of equations that represent the conditions of valid sampling frequencies. There are two main conditions based on the value of N if it is odd or even integer and each have their own set of equations.

In the first case when N is an odd integer as shown in Figure 3.10 (b), the expression is formed by considering that the lower frequency f_l and higher frequency f_h does not overlap with other replicas nor any of the two baseband Nyquist zone borders.

The minimum and maximum sampling frequencies, using f_l and f_h respectively, can be expressed as:

$$-f_h + (N+1)\, f_s > 0 \quad \textbf{(3.20)}$$

$$f_s > \frac{f_h}{N+1} \quad \textbf{(3.20a)}$$

$$-f_l + (N+1)\, f_s < \frac{f_s}{2} \quad \textbf{(3.21)}$$

$$f_s < \frac{2f_l}{2N+1} \quad \textbf{(3.21a)}$$

As for the second case of when N is even, the minimum and maximum sampling frequencies using f_l and f_h can be expressed as:

$$f_l - N\, f_s > 0 \quad \textbf{(3.22)}$$

$$f_h - Nf_s < \frac{f_s}{2} \quad \textbf{(3.22a)}$$

$$f_s > \frac{f_l}{N} \quad \textbf{(3.23)}$$

$$f_s < \frac{2f_h}{2N+1} \quad \textbf{(3.23a)}$$

The RF signal centered at f_c will be down-converted to an intermediate frequency f_{if}. In other words, the f_c-centered bandpass signal will be replicated around $f_c - mf_s$ at each m (where m is a non-zero positive integer) then we will obtain an f_{if} that falls in the range of $0 \ldots \frac{f_s}{2}$. The mathematical relationship between, f_c, f_s and f_{if} can be expressed as:

$$f_{if}\begin{cases} rem(f_c, f_s) & if \left\lfloor \frac{f_c}{f_s/2} \right\rfloor is\ even \\ f_s - rem(f_c, f_s) & if \left\lfloor \frac{f_c}{f_s/2} \right\rfloor is\ odd \end{cases} \quad \textbf{(3.24)}$$

Where $rem(a, b)$ denotes the remainder of a divided by b[47].

3.9.1 Algorithm For Determining The Sampling Frequency For A DRFS Of A Single Bandpass Signal

The first algorithm written is in the case where the input to the ADC is a single band RF signal used to find the valid the sampling frequencies f_s based on the derived constraints equations (3.20) - (3.23). The sampling algorithm is implemented and verified on MATLAB as a code.

The next section explains the single band sampling algorithm architecture as shown in Figure 3.11 and its implementation on GPS L1 band signal in details:

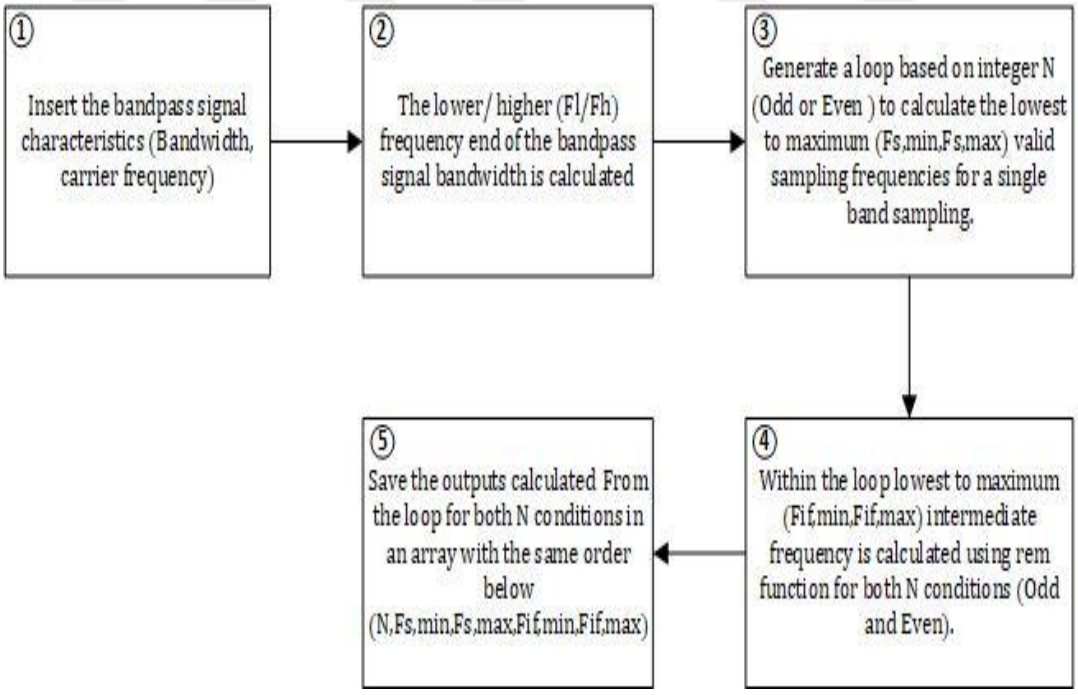

Figure 3.11 Single band sampling frequency calculations algorithm

Step 1: Insert the single-band RF signal center frequency $\boldsymbol{f_c}$ and bandwidth $\boldsymbol{BW}$.

Step 2: Calculate the lower ($\boldsymbol{f_l}$) and higher ($\boldsymbol{f_h}$) end frequencies of the bandpass signal bandwidth from the following equations:

$$f_l = f_c - \frac{BW}{2} \quad \textbf{(3.25)}$$

$$f_h = f_c + \frac{BW}{2} \quad \textbf{(3.26)}$$

Step 3: Start a loop with $\boldsymbol{N}$ as a positive integer that starts at 0 up to $\frac{\boldsymbol{f_l}}{\boldsymbol{2BW}}$. Within the loop, the lower and higher ranges of valid sampling frequencies ($\boldsymbol{f_{s,min}}, \boldsymbol{f_{s,max}}$) are calculated in two cases: in the case $\boldsymbol{N}$ is odd the derived expressions (3.20),(3.21) are used. And in second case when $\boldsymbol{N}$ is even expression (3.22),(3.23) are used.

Step 4: The aliased lower/higher intermediate frequencies ($f_{IF,min}, f_{IF,max}$) are calculated from expression (3.24) for both *N* cases.

Step 5: Finally, the output of the code is saved as an array, where each columns represents a specific value, the first column represents the $\boldsymbol{N}$ values used then the next columns show the proper sampling frequencies ranges from $\boldsymbol{f_{s,min}}$ to $\boldsymbol{f_{s,max}}$ and its intermediate frequencies from $\boldsymbol{f_{IF,min}}$ to $\boldsymbol{f_{IF,max}}$.

The algorithm is used one of the GPS-$\boldsymbol{L_1}$ band signal that has carrier frequency $\boldsymbol{f_c = 1575.42MHz}$, bandwidth $\boldsymbol{BW = 15MHz}$. The signal is bounded between $\boldsymbol{1567.92MHz}$ and $\boldsymbol{1582.92MHz}$, the proper sampling frequencies are extracted by the algorithm and shown in Table 3.1

Table 3.1 GPS L1 band sampling frequencies, sampled output

N	$f_{s,min}$	$f_{s,max}$
52	30.1508 MHz	30.1523 MHz
51	30.440 MHz	30.445 MHz
50	31.03MHz	31.047MHz
49	31.6584 MHz	31.675e MHz
48	32.637 MHz	32.665 MHz.
47	32.9775 MHz	33.0088 MHz
	. . .	
5	287.803MHz	313.584MHz
4	316.584MHz	348.426MHz
3	452.262 MHz	522.64 MHz
2	527.64MHz	627.168 MHz
1	1.05528GHz	1.56792 GHz

The center frequency of $f_c = 1575.42MHz$ with $BW = 15MHz$ Bandwidth the data is bounded between $1567.92MHz$ and $1582.92MHz$, the various sampling rates are extracted by the algorithm as shown in Table 3.1, this tell us that permissible sample rate may vary in ranges of sampling frequencies. All spectra for sampling rates that are shown are above $2BW$.

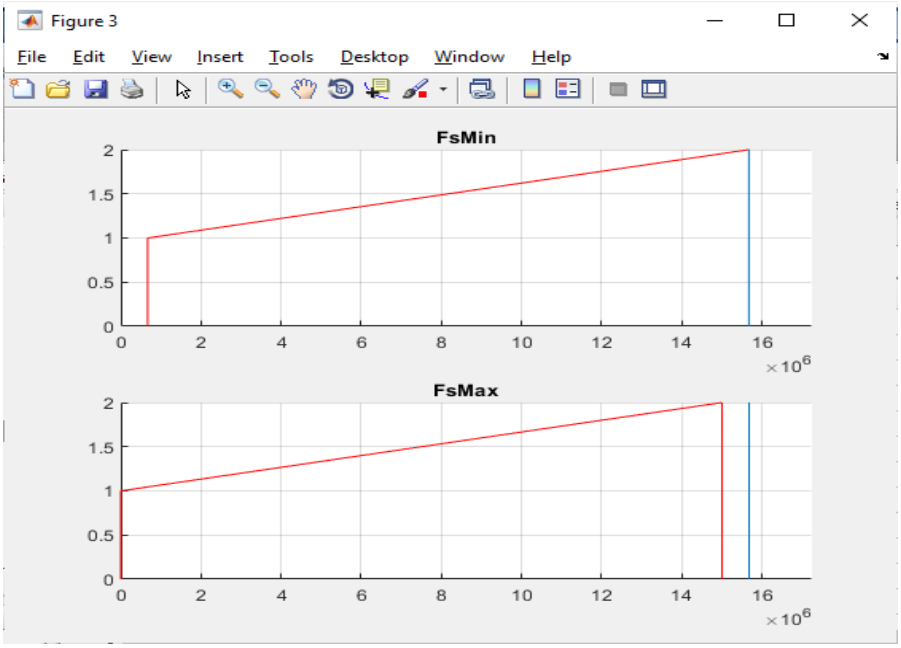

Figure 3.12 Plot of a sampled bandpass signal using one of the f_s values in Table 3.1

The outcome of the algorithm is used to plot the resultant spectrum of the sampled signals and the constraints of obtained and is checked to be fulfilled. The validity of this check is depicted in Figure 3.12**,** where the range from $f_{s,min} = 31.03MHz\ to\ f_{s,max} = 31.047MHz$ is used on the GPS L1.

3.9.2 Algorithm for Determining the Sampling Frequency for a DRFS of Multiple Bandpass Signals

In case 2 There have been many approaches over the years to find the most suitable way to obtain the optimal and minimum bandpass sampling frequency for multi-band signals with different methods, Akos [46] found conditions to obtain the sampling frequency, but its complexity is based on computing cost with more power consumption. In [48] Choe approached with same and inverse placement between input and output signals to a find sampling frequency with minimized computing cost. In [41], Tseng and Chou proposed an algorithm that finds the ranges of valid sampling frequencies using formulas that are extracted from the boundary frequencies of each bandpass signal.

The multi-band algorithm we developed and implemented on MATLAB dramatically decreased the number of computational costs compared to [41,42,48]. It is considered to be a flexible, more robust way to find valid sampling frequency ranges and doesn't demand deriving complicated constraints equations for each sampling condition unlike [41,44,48] and their complex solutions. The approach we took involves using the valid sampling frequency ranges of each GPS L1, L2, and L5 band obtained from the single-band algorithm to find the overlapping f_s ranges between them that exceed twice the total bandwidth of the bands, afterwards the common ranges are filtered based on the aliasing conditions of down-converted signal.

The next part clarifies the algorithm architecture we developed and implemented in MATLAB to find the valid sampling frequencies of multiple bandpass signals GPS L1, L2, and L5 bands starting by its operation steps.

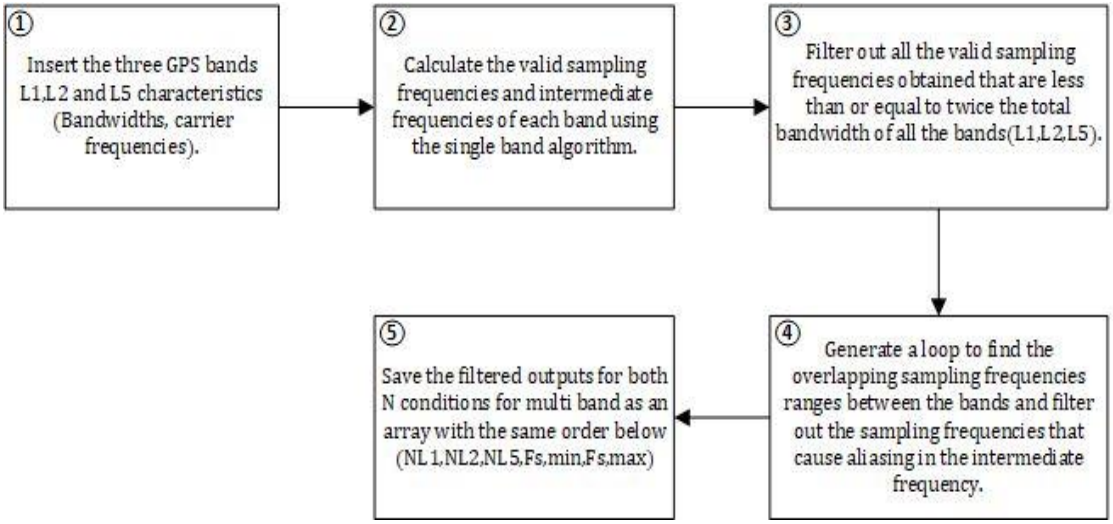

Figure 3.13 Multi-band sampling frequency calculations algorithm

Step 1: Insert the characteristics of the three RF signals, their center frequencies $\boldsymbol{f_{cm}}$, and bandwidth $\boldsymbol{BW_m}$ where $\boldsymbol{m}$ indicates the index of the RF single.

Step 2: The three bands proper $\boldsymbol{f_s}$ values were calculated independently using the single band algorithm in section 3.9.1. The first filtering condition applied is following the Nyquist theorem where each obtained $\boldsymbol{f_s}$ value that fall under twice the total bandwidth $\boldsymbol{BW_{tot} = BW_1 + BW_2 + \cdots}$ are removed.

Step 3: A loop is generated to filter all obtained $\boldsymbol{f_s}$ values through comparing each $(\boldsymbol{f_{s,min}}, \boldsymbol{f_{s,max}})$ of each band with the other bands to remove $\boldsymbol{f_s}$ values that are not overlapping between the bands. The first condition can be set where $\boldsymbol{f_{s_1,min}}$ should be higher than or equal to $\boldsymbol{f_{s_2,min}}$ and $\boldsymbol{f_{s_3,min}}$, then it should also be lower or equal to $\boldsymbol{f_{s_2,max}}$ and $\boldsymbol{f_{s_3,max}}$. Using several conditions for each band as previously explained will allow us to find overlapping $\boldsymbol{f_{s,min}}$ and $\boldsymbol{f_{s,max}}$ between all the three bands.

Step 4: The second filtering conditions within the loop indicates that the spacing between f_{IF_1}, f_{IF_2}, f_{IF_3}, 0 and $\frac{f_s}{2}$. The intermediate frequencies of each band compared to the other should be bigger than half the total bandwidth of themselves, each lower end frequency $(f_{IFm} - BW_m/2)$ should be bigger than 0, and higher end frequency $(f_{IFm} + BW_m/2)$ should be smaller than $\frac{f_s}{2}$. These conditions are to make sure there

is no aliasing occurring and remove the obtained sampling frequencies $(f_{s,min}, f_{s,max})$ that allow aliasing.

$$f_{IF} = (-1)^N * f_c - (-1)^N * (f_{s,min} + abs(N - 20) * f_s) \quad \textbf{(3.27)}$$

Step 5: The sampled data is saved into an array that contains the odd and even integers $\boldsymbol{N_{L_1}}$,$\boldsymbol{N_{L_2}}$,$\boldsymbol{N_{L_3}}$, and sampling frequencies $\boldsymbol{f_{s,min}}$ to $\boldsymbol{f_{s,max}}$.

Following the multiple-band algorithm, we considered 3 GNSS signals in GNSS bands (L_1, L_2, L_5) with their carrier frequencies$f_{c1} = 1575.42MHz$, $f_{c2} = 1227.6\,MHz$, $f_{c3} = 1176.45\,MHz$ and bandwidth $BW_1 = 15MHz$, $BW_2 = 11MHz$ $BW_3 = 12.5MHz$. The algorithm extracts the proper sampling frequencies for these three bands individually, The proper sampling ranges found in Table 3.2. The BW_{tot} of GPS bands (L_1, L_2, L_5) equals to $38MHz$, indicating that the $(f_{s,min}, f_{s,max})$ values showed be $f_s \geq 76MHz$.

Table 3.2 GPS L1,L2 and L5 bands vaild sampling frequencies obtained by Matlab

$\boldsymbol{N_1}$	$\boldsymbol{N_2}$	$\boldsymbol{N_3}$	$\boldsymbol{f_{s,min}}$	$\boldsymbol{f_{s,max}}$
10	8	7	$\boldsymbol{151.7542MHz}$	$\boldsymbol{151.7625\,MHz}$
9	7	7	$\boldsymbol{158.292\,MHz}$	$\boldsymbol{158.95\,MHz}$
7	5	5	$\boldsymbol{221.036\,MHz}$	$\boldsymbol{222.2\,MHz}$
6	5	5	$\boldsymbol{226.131\,MHz}$	$\boldsymbol{231.040\,MHz}$
. . .				
3	2	2	$\boldsymbol{493.24MHz}$	$\boldsymbol{522.64\,MHz}$
2	2	2	$\boldsymbol{527.64MHz}$	$\boldsymbol{585.10\,MHz}$
2	2	1	$\boldsymbol{591.35\,MHz}$	$\boldsymbol{611.05\,MHz}$
2	1	1	$\boldsymbol{633.168}$MHz	$\boldsymbol{780.13MHz}$
1	1	1	$\boldsymbol{1.05528\,GHz}$	$\boldsymbol{1.1702\,GHz}$

The outcome of the Multi-band algorithem is used to plot the resultant spectrum of the sampled signals (GPS L1,L2, and L5) which prove the validity of the algorithem as depeicated in Figure 3.14 where $\boldsymbol{f_s}$ ranges from $\boldsymbol{151.7542MHz}$ to $\boldsymbol{151.7625\,MHz}$ is used from Table 3.2.

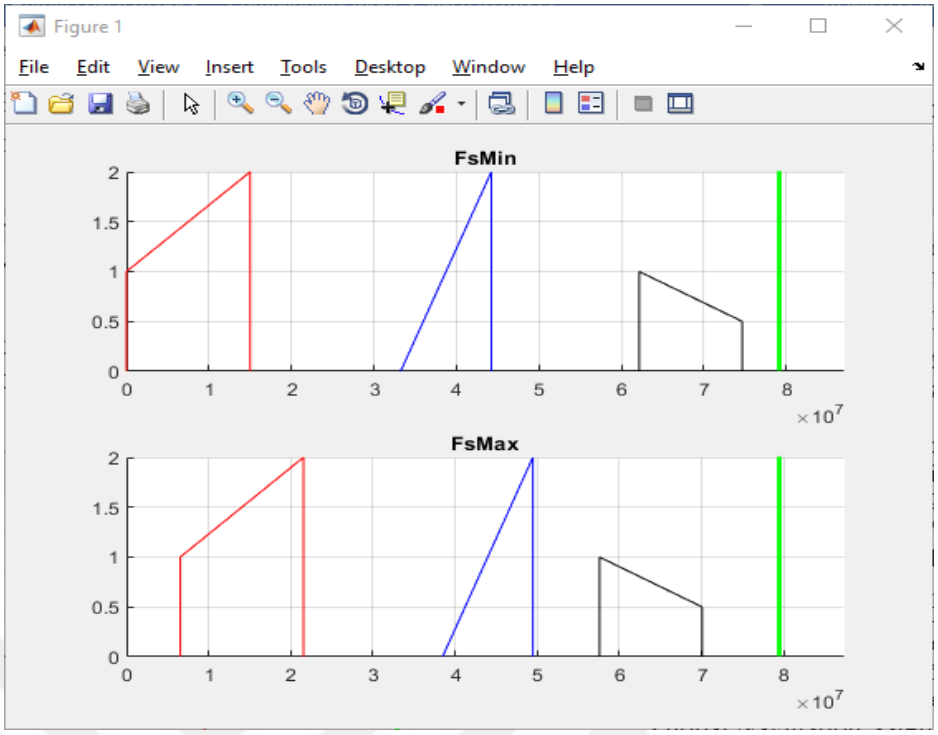

Figure 3.14 Plot of three bands sampled bandpass signals using one of the f_s values extracted in Table 3.2

We can conclude that the proposed algorithm results in the ranges of valid bandpass sampling frequencies for complex signals in terms of bandwidths and band positions of the single-bandpass and multi-bandpass RF signals. Compared to other published approaches [44,45] on bandpass sampling, we were able to acquire valid sampling frequency ranges much easier, the obtained ranges are much wider.

3.9.3 Noise Folding

Noise folding is defined as the accumulation of noise from aliased frequencies on top of the desired band of interest at f_{if} because of the sampling process where the spectrum shifting accrue as shown in **Figure 3.15**. The total noise that gets folded is mainly generated by the hardware components of the receiver (Amplifiers, Antenna … etc.) and this noise is known to be an Additive White Gaussian Noise (AWGN) if we assume the amplifier and flicker noise lower than thermal noise[49].

The practical implementation of our multi-GNSS DRFS receiver demands us to consider noise folding as an important factor for two main reasons. The first reason is that the number of amplifications that we have in our design after the BPF and before the ADC will amplify the out-of-band noise that will be folded or aliased into the sampled signal of interest and degrade the SNR. Adding a second BPF directly before the ADC will suppress the out-of-band noise and can be a proper solution to the problem.

The second reason is low/medium level sampling used in our design can cause a tradeoff with noise. For example, setting a lower sampling frequency will increase the amount of noise folding that is expected to accrue and decrease the SNR. This tradeoff is inevitable, the best solution is to find a middle ground for proper sampling frequency with an acceptable SNR[3].

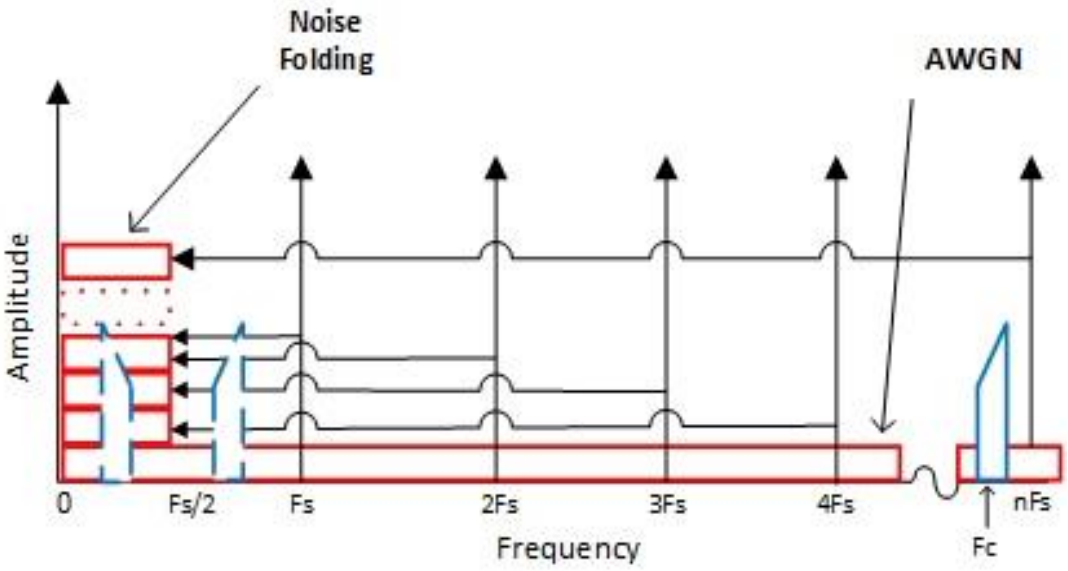

Figure 3.15 Noise folding illustration

The aliased noise components are proportional to the used amplification stages and get added to one another creating noise by a factor of N times the normal noise in the Nyquist band in both negative and positive frequencies as shown in

Figure 3.16 Noise folding of both negative and positive . Where N is an arbitrary positive integer ensuring that the sampling frequency ranges $fs > 2BW$ [49].

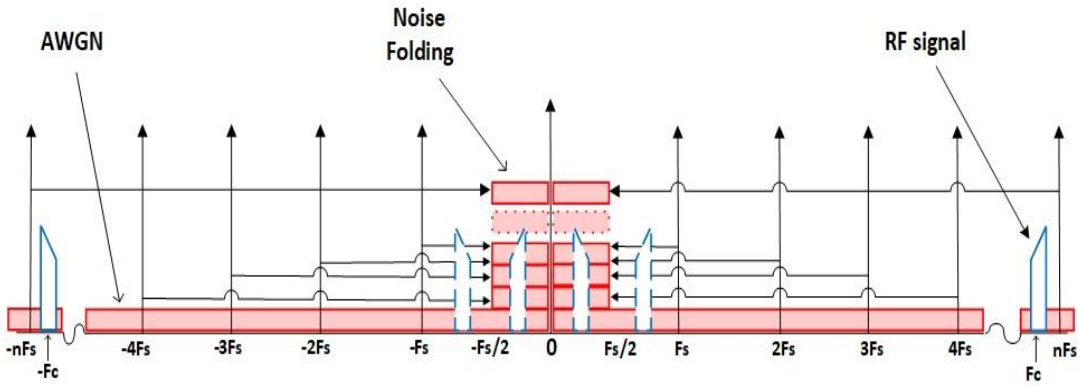

Figure 3.16 Noise folding of both negative and positive frequencies

To calculate the noise folding we can consider the $\boldsymbol{N_i}$ as in-band noise, $\boldsymbol{N_o}$ as out of band noise and $\boldsymbol{N}$ as a sampling integer. Mathematically, we quantify that the total noise to be considered is:

$$N_i + \sum N_o = N_i + 2(N-1)N_o \qquad \textbf{(3.28)}$$

It is very important to suppress the out of band noise $\boldsymbol{N_o}$ and this can be done by adding a bandpass filter prior to the ADC [49].

3.10 ADC Noise Considerations

There are several factors that can impact the overall system operation of the ADC in a DRFS-based system and can limit its performance. These factors include quantization noise, thermal noise, aperture jitter. These factors will be discussed in detail below[50].

3.10.1 Quantization Noise

Analog to digital converters (ADCs) perform an amplitude quantization of an analog input signal into binary output words of finite length with specific range of bits. Due to this conversion some signal non-linearities are expected. These nonlinearity presents itself as a wideband noise called quantization noise. In other words,

quantization noise is the rounding error between analog input voltage to the output digitized value after the ADC therefore, its increase limits the ADC's dynamic range and performance.

From the conversion process, we can say that each single digital output corresponds to a range of analog input amplitudes (voltages). This range equals the least significant bit (LSB):

$$\text{LSB}_{size}(\text{V}) = \frac{\text{FSR}}{2^n} \quad \textbf{(3.29)}$$

FSR represent the value of the full-scale range in volts and n is the number of bits of the ADC's output (aka ADC resolution) [51].

the plot of an ADC's ideal transfer function (unaffected by offset or gain error). The transfer function extends from the minimum input voltage to the maximum input voltage horizontally and is divided into several steps based off the total number of ADC codes along the vertical axis. This plot has 16 codes, or steps, representing a 4-bit ADC.

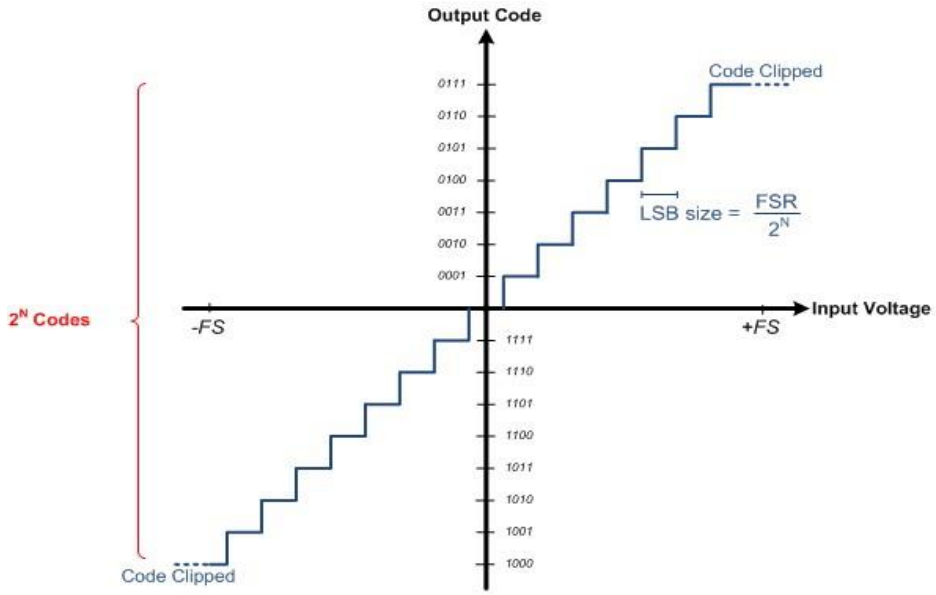

Figure 3.17 An ADC's ideal transfer functions[34]

In direct radio frequency receiver design we need to measure the quantization noise and see its effects starting by Deriving it's general expressions, [52] estimated a sampled signal with an amplitude of -1 to 1 and an $\boldsymbol{n}$ bit quantization used, the error value is possibly uniformly distributed in the range from $-\boldsymbol{2^{-n}}$ to $-\boldsymbol{2^{n}}$, the power formula is expressed as:

$$var\big(e(i)\big) = \frac{2^{-2n}}{3} \tag{3.30}$$

Where the error of $\boldsymbol{i}$-th sample is $\boldsymbol{e(i)}$. To derive the $\boldsymbol{SNR}$ due quantization noise, we can consider the root mean square (RMS) power of a signal is $(\boldsymbol{V_{RMS}})^{\boldsymbol{2}} = \boldsymbol{1/2}$ then the $\boldsymbol{SNR}$ is expressed below:

$$SNR_{quant} = \frac{1/2}{2^{-2n}/3} = \frac{3}{2}2^{2n} \tag{3.31}$$

Considering white noise model is required when it comes to quantization noise and thus $\boldsymbol{PSD}$ noise can be written as:

$$PSD_{quant}(f) = \frac{P_{quant}}{f_s} = \frac{P_{signal}}{SNR_{quant}.F_s} = \frac{2P_{peak}}{3f_s 2^{2n}} \tag{3.32}$$

$\boldsymbol{P_{peak}}$ is the most critical quantity in quantization, instead of the average power of the signal $\boldsymbol{P_{signal}}$ therefore we have substituted $\boldsymbol{P_{signal} = P_{peak}}$ .Based on the used sampling rate $\boldsymbol{f_s}$ white noise naturally falls over the whole bandwidth.

3.10.2 Thermal Noise

Thermal noise is a constant accruing theme when it comes to electrical components due to the physical movement of charge inside electrical conductors. Thermal noise corresponds to the ambient noise present at the receiver antenna level, it is assumed to be white and gaussian with PDS equal to:

$$N_0 = KT_s \quad \textbf{(3.33)}$$

Where K is Boltzmann constant.

T_s is the system noise temperature, dependent upon the front-end architecture (filters and *Low Noise Amplifiers* (LNA)) and defined through the Friis formula.

3.10.3 The Sampling Jitter Noise

Direct RF sampling architecture has an edge over other architectures where it can sample many signals simultaneously with a single RF front-end if the optimal sampling frequency is selected. This advantage comes with a tradeoff such as the need for an analog to digital converter with higher sampling frequency in the megahertz level which leads to faster digital processing and more sensitivity to sampling jitter.

Jitter sampling is a random change in the periodic signal over a period in the time domain and phase noise in the frequency domain, the addition of noise because of jitter to the sampled signal will reduce the signal to noise ratio (SNR). It should be considered in our multi-GNSS receiver design since it requires a high sampling which renders the SNR more susceptible to jitter noise[2].

There are two sources of jitter: the sampling clock and the ADC itself. The sampling clock is generally supplied by a phase lock loop (PLL) or any external source like an oscillator is responsible for the sampling clock jitter. Thermal noise is considered the internal cause of extra jitter within the ADC which limits some of the usable bits of the ADC [53]. Since we cannot measure the effect of jitter sources individually, it is typical practice to measure the total jitter by taking the root mean square of the combination of both jitter sources as a general formula.

$$\sigma_\tau = \sqrt{(\sigma_{jitter,ext})^2 + (\sigma_{jitter\_ADC})^2} \quad \textbf{(3.34)}$$

To measure the maximum allowable jitter noise, we can start by using the Binary Phase Shift Keying signal like the one generated by the GPS satellites for the GPS L1 C/A signal as an example, the noise power generated by jitter expression developed by [54] shown below:

$$N_\tau = A^2\left(\frac{\sqrt{2}}{\sqrt{\pi}}\sigma_\tau f_d + 2\pi^2 {f_c}^2 {\sigma_\tau}^2\right) \quad \textbf{(3.35)}$$

In equation (3.35) where N_τ is the noise power generated by the jitter, σ_τ is the total system jitter, f_d is the BPSK data frequency, f_c is the carrier frequency of the GNSS signal at ADC input, A is the constant carrier amplitude of the incoming BPSK signal at ADC input. The expression we can clearly show that the higher the sampling frequency the higher the noise power generated by jitter will be.

The next step of finding the maximum jitter noise is to calculate signal to jitter ratio (SJR) of the sampled signal of interest from equation (3.35), signal to jitter ratio is defined below where the total signal power (S) is considered the signal's carrier power $\frac{A^2}{2}$:

$$SJR = \frac{S}{N_\tau} = \frac{\frac{A^2}{2}}{A^2\left(\frac{\sqrt{2}}{\sqrt{\pi}}\sigma_\tau f_d + 2\pi^2 {f_c}^2 {\sigma_\tau}^2\right)} \quad \textbf{(3.36)}$$

In [54] Dempster proposed an approach to restricting The jitter noise power to be 10dB down from the thermal noise power (N_{th}) to constrain noise power generated by the jitter, the restriction is written below:

$$N_\tau \geq 10\frac{S}{N_{th}} \quad \textbf{(3.37)}$$

Finally from the limitation rule that has been proposed (3.37), we can calculate the maximum jitter noise σ_τ knowing that $N_{th} = KTB_d$, B_d is the bandwidth of GNSS signal of interest, K is Boltzmann constant $(1.39 \times 10^{-23} J.K^{-1})$ and T is the noise temperature of the GNSS receiver, solving for σ_τ from SJR equation (3.21) the jitter constraint is :

$$\sigma_\tau \leq \frac{\sqrt{\frac{80{f_d}^2 S}{\pi kTB_d} + 16\pi^2 {f_c}^2} - \sqrt{\frac{80{f_d}^2 S}{\pi kTB_d}}}{8\pi^2 {f_c}^2 \sqrt{\frac{10S}{kTB_d}}} \quad \textbf{(3.38)}$$

Equation (3.38) is a measurement for the maximum allowable jitter noise for the GPS L1 C/A signal.

CHAPTER 4

MULTIPLE GNSS DIRECT RF SAMPLING RECEIVER CIRCUIT DESIGN AND IMPLEMENTATION

4.1 Introduction

The previous chapters have established a theoretical framework on the design of direct RF sampling receiver for GNSS signals. The receiver first part is the RF front-end, which is the subject of this chapter. The chapter starts by explaining the general design requirements of the DRFS receiver components, then followed by selection of the amplifiers, bandpass filter, and the ADC. Finally, The proposed DRFS receiver design is simulated in awr design environment (AWR) simulation program to analyze and validate the theoretical framework done with the simulation output.

4.2 Technical Design Specifications

4.2.1 General Architecture of the DRFS Receiver

The general architecture of the direct RF sampling receiver consists of two main separate parts: the RF signal chain and the digital signal processing.

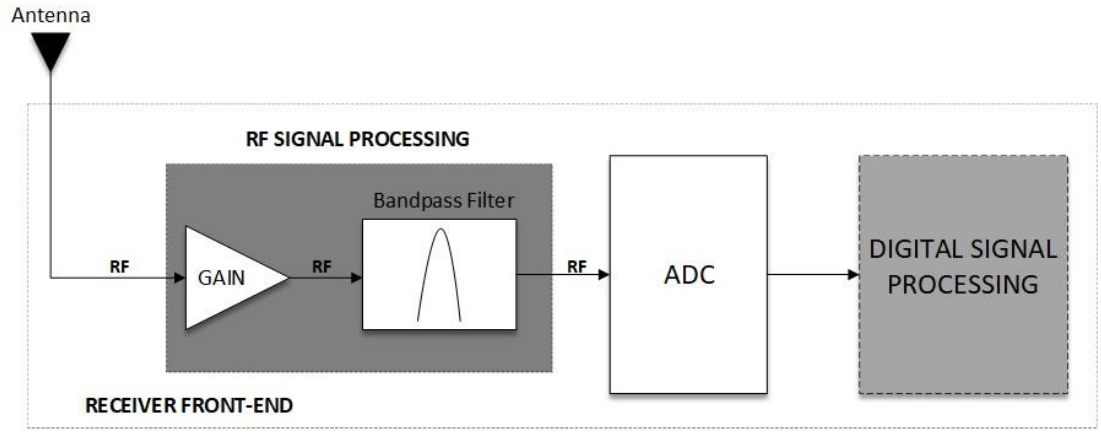

Figure 4.1 General Architecture of Direct RF sampling receiver

The RF signal chain is the amplification and filtering stages of the signal before sampling. Because of the extremely low power level of GNSS signals, as shown in

Table 2.2, it is necessary to amplify the GNSS signals prior to sampling. In addition, as demonstrated in bandpass sampling explained in section 3.8, it is necessary to filter the GNSS band of interest as narrow as possible in order to avoid high level of noise folding on the desired signal. while the ADC converts the GNSS band of interest in order to reduce it to an intermediate frequency.

4.3 Initial Assessment of Required RF Amplification and Filtering

The amplifiers in the receiver RF chain must have sufficient gain to amplify the GNSS signals to the full voltage scale of the ADC to obtain a well sampled signal. As presented in Table 2.2, GNSS signals have ground power levels of approximately -160 dBW. This low power implies that these signals are below the thermal noise level generated by the receiver, known as the noise floor. This noise is white Gaussian noise that is primarily thermal in nature [42]. the noise power depends only on the limited bandwidth used and the temperature of the receiver components as seen previously in equation (3.33).

Similar architectures; Psiaki [43] used 95 dB gain, Akos [27] used 90dB gain and Guillaume Lamontagne [2] used 100 dB gain. Based on that, we estimated the needed gain for the receiver RF chain to be 100 dB over a wide band (from 1.1 GHz to 1.7 GHz approximately) to cover all GNSS signals.

When it comes to designing receiver RF chain amplification, it is very crucial that the last amplifier used prior to the ADC to be controllable to configure its gain to reach the full voltage scale of the ADC. This kind of amplifiers is called Variable Gain Amplifier (VGA).

Signal filtering is necessary before sampling to avoid the aliasing of the noise on the information band. However, there will always be some noise power added to the signal as explained is section 3.9.3, despite of the quality of the filtering. This noise decreases the SNR of the sampled signal. Because there is no theoretical limit for this noise, it is important to impose an arbitrary limit this noise. In that regard, we choose to limit the power of the noise folded over the GNSS signal to 10 dB below the GNSS signal. Since most GNSS signals are about 30 dB below thermal noise [54],

the out of band noise folded onto the signal must be attenuated by 40 dB relative to the signal in the filter passband. The RF filter must also have the most linear phase variation possible in frequency in order to keep the phase coherence between the different GNSS signals.

4.4 Selection of Key Components and Parameters

4.4.1 Amplification Selection

Based on the initial assessment of the required amplification to reach the full voltage scale of the ADC we will require a total of 100dB amplification stage starting with a Low Noise Amplifier (LNA), several Block Gain Amplifiers (BGA) and a Variable Gain Amplifier based on the DRFS architecture in Figure 1.2**.**

All active components in a receive chain, particularly amplifiers, add thermal noise to the signal passing through them. The effects of this noise in the receiver chain determine the signal detection threshold of the receiver [26].

Knowing that GNSS signals are below the thermal noise floor, it is important not to further degrade their SNR with amplifiers that add a lot of noise to the signal. We therefore define a figure of merit, called the noise figure as mentioned in 3.7.1, which represents the ratio of the SNR at the input of a component to the SNR at its output. The calculation of noise figure is presented in equation (3.5)[26].

Based on equation (3.8), the total noise figure of a receiving chain depends heavily on the first component in the chain. If this component is selected to be with a low noise figure and high gain, the total noise figure will be low. Therefore, low noise amplifier (LNA) is generally used at the beginning of any receive chain. For passive components, the absolute value of the insertion loss is taken as the noise figure.

There are many LNA components that can amplify the GPS L1 C/A band in the market, to choose the proper LNA we need to consider that its band of operation to be wide, its gain to be more than 20dB, its noise figure to be less than 2dB, its input return loss to be less than -10dB, and its input impedance Zo to be 50 Ω. Based on those research criteria we selected ADL5523 LNA from analog devices to be the

LNA of choice. Its characteristics are explained in So far, we had selected an LNA and VGA with a total gain of 21.5dB ± 15.46dB from 100 dB gain required that leaves us with a 78 dB additional gain, this gain can be provided using a cascade of two Block Gain Amplifiers (BGA), these amplifiers selection is based on the same criteria of the LNA except for a relaxed noise figure. The BGA2869 from NXP is selected, its characteristics are explained below.

Table 4.1.

Based on section 4.3, we are required to use a Variable Gain Amplifier (VGA) that allow us to adjust the signal amplitude to reach the full scale of the ADC, having a control range of 2dB is considered efficient. After research we found the HMC625BLP5E to be the perfect fit. The component characteristics are explained in Table 4.1.

So far, we had selected an LNA and VGA with a total gain of 21.5dB ± 15.46dB from 100 dB gain required that leaves us with a 78 dB additional gain, this gain can be provided using a cascade of two Block Gain Amplifiers (BGA), these amplifiers selection is based on the same criteria of the LNA except for a relaxed noise figure. The BGA2869 from NXP is selected, its characteristics are explained below.

Table 4.1 Main characteristics of LNA, BGA , VGA

CRITERIA	**VALUE**		
Amplifiers	**LNA(ADL5523)**	**BGA(BGA2869)**	**VGA(HMC625BLP5E)**
Operation Band	$400MHz\ to\ 4\ GHz$	$250MHz\ to\ 2.2\ GHz$	$DC\ to\ 5\ GHz$
Noise Figure	0.8 dB	3.1dB	6dB
Gain	21.5 dB	31.7dB	-13.5 to +18 dB gain (0.5dB step gain control)
Input return Loss	-8 dB	18dB	15 dB
Load Impedance	50 Ω	50 Ω	50 Ω

4.4.2 Signal Splitter/Combiner Selection

Based on the general multi-GNSS direct radio frequency receiver in Figure 1.3, splitter and combiner component are required thus allowing us to split the main the RF signal into three RF signals to be filtered with three different bandpass filters that corresponds to each GPS L band signal, then combined back again into single RF signal. The selection criteria of splitter/combiner are :

1. Minimum operation band from 1164 MHz to 1610 MHz .
2. High isolation.
3. As low insertion loss as possible.

Based on these criteria we selected SCN-3-16+ from Mini-circuits and its characteristics are below:

Table 4.2 Main characteristics of Combiner/splitter

CRITERIA	**VALUE**
Split/Comb	**SCN-3-16+**
Operation Band	$950MHz\ to\ 1600MHz$
Isolation	20 dB
Insertion loss	0.6 dB
Load Impedance	50 Ω

4.4.3 GPS L Bands RF Filtering Selection

There are many Band Pass Filters (BPF) available in the market for the L1 C/A, L2 and L5 GPS signal. The following criteria were considered in order of importance to select these components:

1. Minimum bandwidth of 15.3MHz for GPS L1, 11MHz and 10.3 MHz for GPS L5 at -3dB.
2. Minimum attenuation in the pass band.
3. 50 Ω input and output impedance matching.

The filters selected after research are the SF1186B-2(GPS L1), SF2208E(GPS L2), and SF2388E(GPS L5), Surface Acoustic Wave (SAW) type, from the RFM company. These filters have the characteristics shown in Table 4.4.

Table 4.3 Main characteristics of the GPS L bands filters

CRITERIA	**VALUE**					
Filters	**SF1186B-2(L1)**		**SF2208E(L2)**		**SF2388E(L5)**	
Operation Band	1,567.77 MHz to 1,583 MHz		1217 MHz to 1237 MHz		1166.45 MHz to 1186.45 MHz	
Bandwidth	15.3 MHz		20 MHz		$20MHz$	
Attenuation reference at	$1500MHz$	$1640Mhz$	$1177MHz$	$1290Mhz$	$1121.45Mhz$	$1231.45MHz$
Attenuation	$52.7dB$	$59.1dB$	$21.6dB$	$36dB$	$42dB$	$45dB$
Insertion Loss	$2.68dB$		$0.95dB$		3.3 dB	
Load Impedance	50 Ω		50 Ω		50 Ω	

As shown previously the selected filters follows the constraints provided, each bandwidth is considered more than enough to capture its corresponding GPS L information signal.

4.4.4 ADC Selection

The selection of the analog to digital converter can be based on several factors to obtain the maximum performance, The selection criteria is shown in the table below .

Table 4.4 ADC selection Criteria

Criteria	**Value**
Minimum sampling frequency	151.7 MHz based on Table 3.2
Minimum number of bits	3 bits
Maximum input frequency	1609.6 MHz

The criteria of mentioned in the previous table are based on the bandpass sampling algorithm in section 3.9 used to select the minimum sampling frequency required to sample the GNSS bands, and the maximum input frequency and signal amplitude that ADC that endure. The AD9680 ADC from analog devices is selected, the high speed AD9680 is used in an FMC evaluation board FMCDAQ2 that uses JESD204B coded serial digital outputs and can be connected to an FPGA for data acquisition. The details of the AD9680 are explained below.

Table 4.5 General characteristics of the AD9680

Characteristics	**Values**
Maximum sampling frequency	1.25 $GSPS$
Minimum sampling frequency	300 $MSPS$
Resolution (number of bits)	14 bits
Maximum input frequency	2 GHz
FSR	2 Vp-p
ENOB	10.8 bits
SNR	60.5 dBc
Power consumption	1.65 w per channel (3.3w for dual channels)

4.4.5 The DRSF Final Architecture

After following the small steps of selection criteria, a complete direct radio frequency receiver front end presented and shown in Figure 4.2.

The LNA occupies the first position in the receiving chain to minimize the SNR degradation of the amplified signal. The next three gain block were distributed throughout the receiver, the first one is just after the LNA, and the last two positions right before the variable gain amplifier which adjusts its amplitude to the full scale of the ADC. Three filters are mainly used, and they are located between the two splitters/combiners components where it splits the main RF line transmitted from the first gain block into three separate filters lines for each GPS L band then combine the separate signals into one RF line with three GPS L1,L2, and L5 filtered signals.

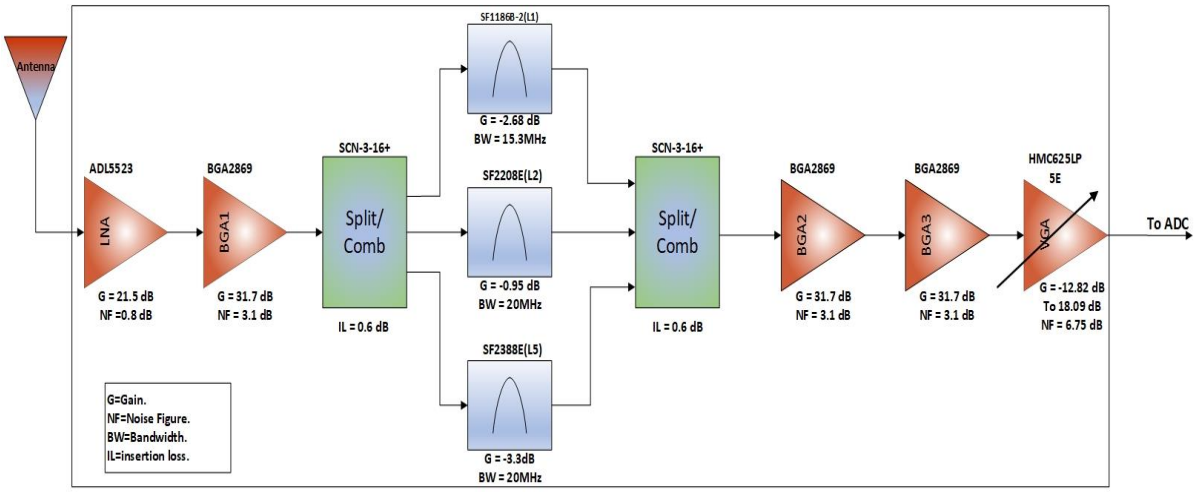

Figure 4.2 Final RF signal processing chain

4.5 Simulation of the Overall DRFS architecture in AWR Design Environment

4.5.1 Description of the Simulation and the Models Implemented

The objective of the AWR simulation is to validate the DRFS receiver architecture with the ADC sampling frequency calculated in section 3.9, and design consideration for example, Noise figure, SNR, and dynamic range . To do this, we seek to generate an L1 C/A GPS to simulate the satellite transmission process. The first step of the simulation is to generate PRN codes for SV #2,#3,#4,#5 using basic GPS CA code generator as shown in Figure 4.3, 4 generators are simulated with different delay that correspond with each satellite.

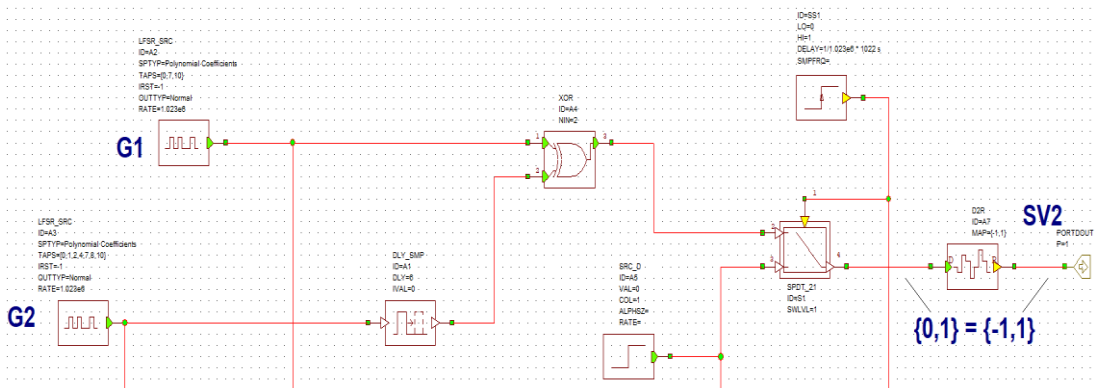

Figure 4.3 GPS CA code generator

The second part is generating a navigation signal for each SV at 1.023Mhz in Figure 4.4 with data rate of 50 bps and combine it with the corresponding CV code, followed by a Binary Phase-shift keying modulation (BPSK) at a carrier frequency of 1575.42 MHz in Figure 4.5.

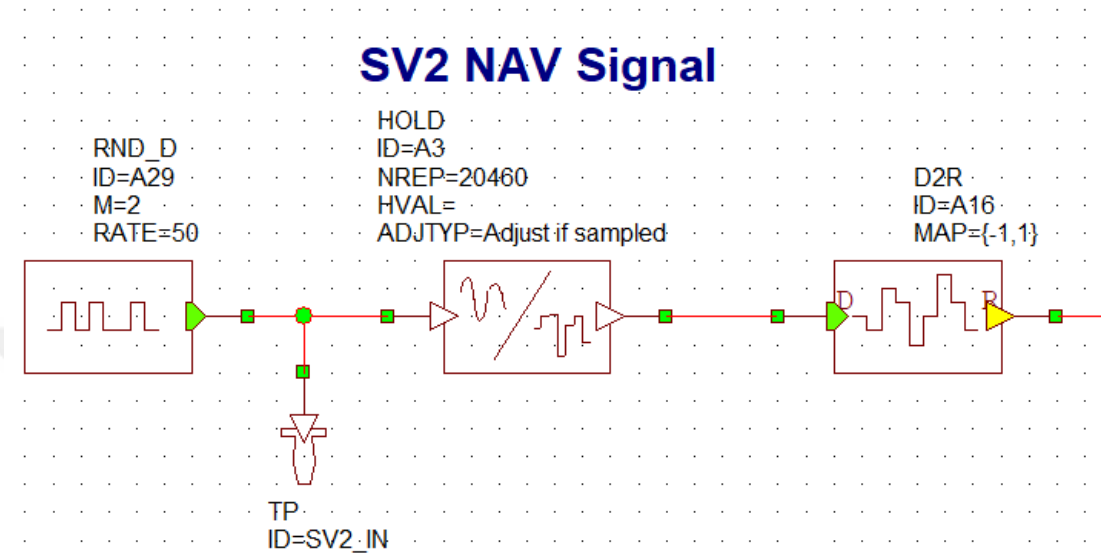

Figure 4.4 Navigation signal generation

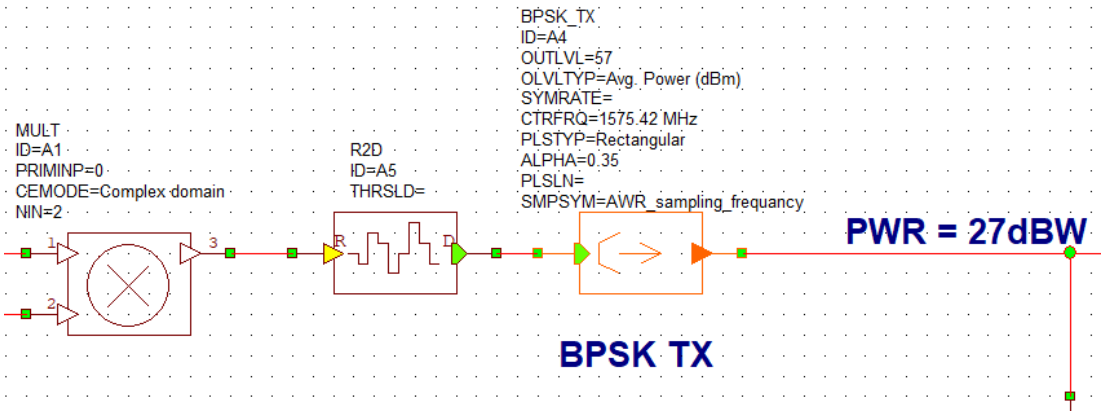

Figure 4.5 BPSK TX of single satellite signal (CV code+ navigation)

After BPSK modeling each satellite signal (SV #2,#3,#4,#5), a combiner merges all the satellite signals and transmit them for a distance of 21000 km using an antenna that simulates the standard GPS satellites antenna.

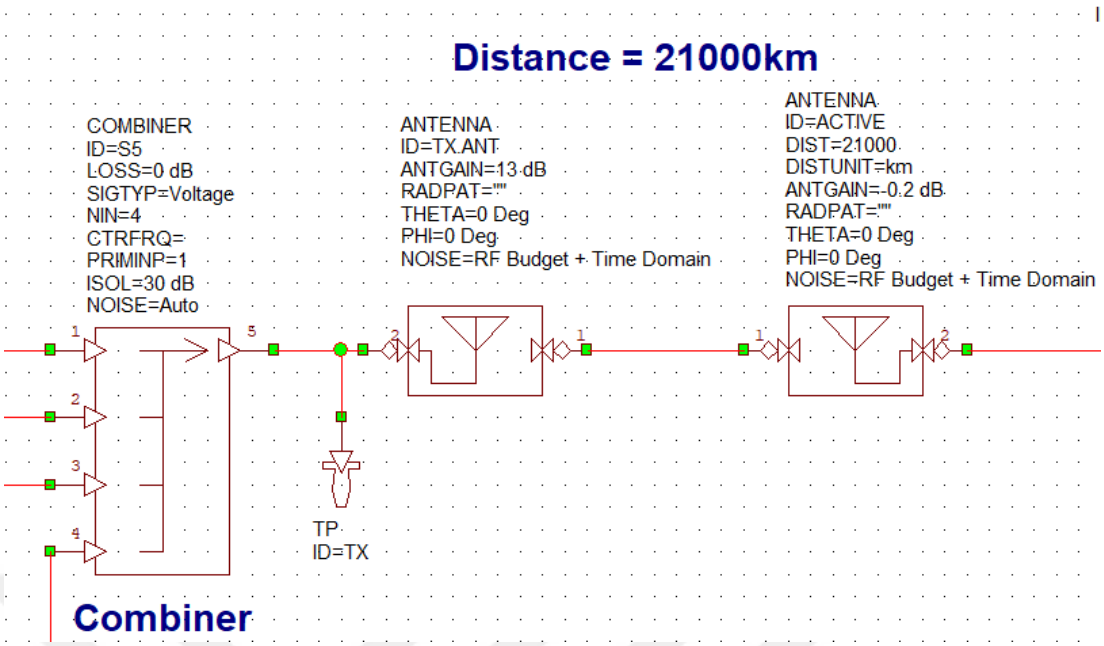

Figure 4.6 Transmitter of the signal over 21000km distance

Then following the final signal processing diagram in Figure 4.2, we implemented the direct radio frequency sampling receiver by adding the recommended amplifiers and bandpass filter for GPS C/V L1 in Figure 4.7 followed by the sampling process with an ADC of a sampling frequency that is obtained in section 3.9.1.

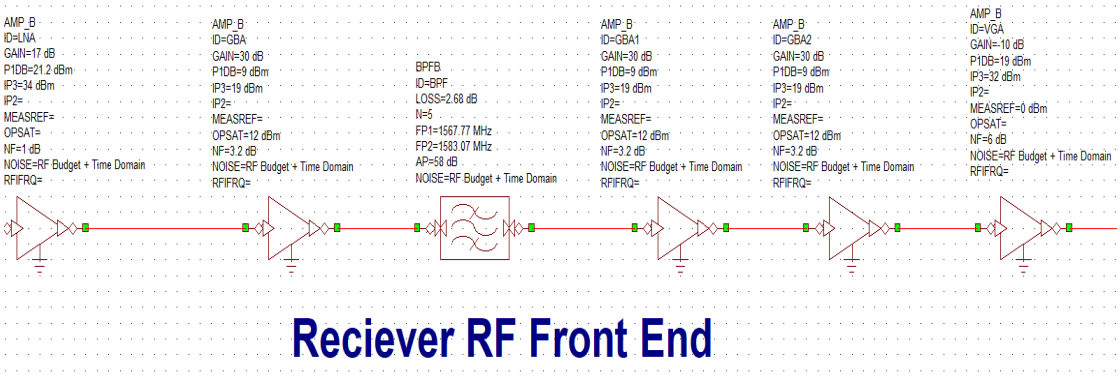

Figure 4.7 Direct RF sampling receiver

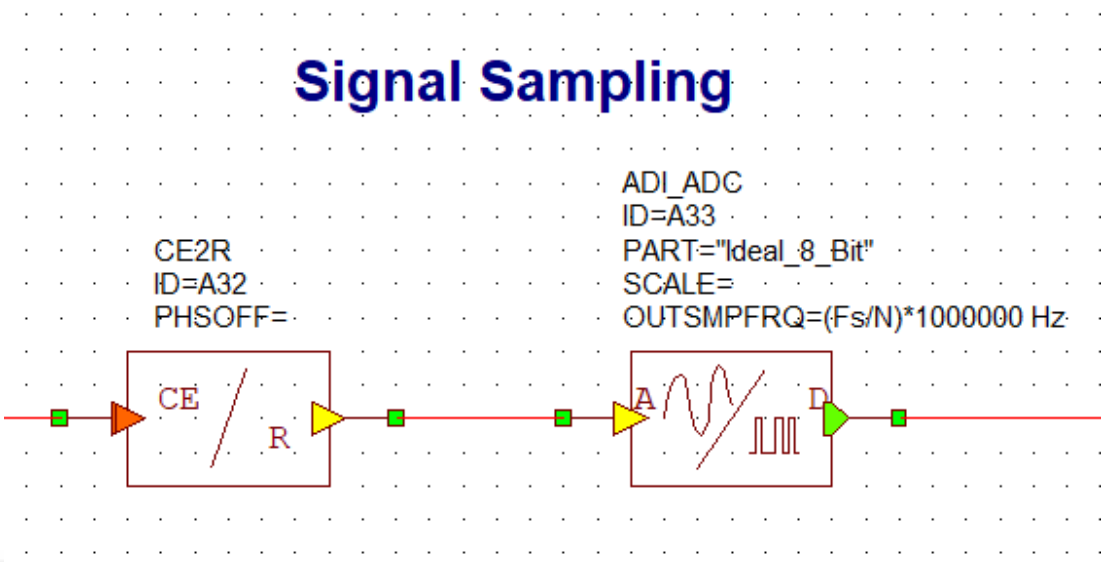

Figure 4.8 ADC sampling

4.5.2 Simulation Results Analysis

Based on AWR simulation that has been presented above, a full spectrum analysis is done starting by the transmitted satellite signal from diagram Figure 4.7 the transmitted signal has a propagating power of 63dB at a 1575.42 MHz center frequency (GPS C/V L1) shown in Figure 4.9.

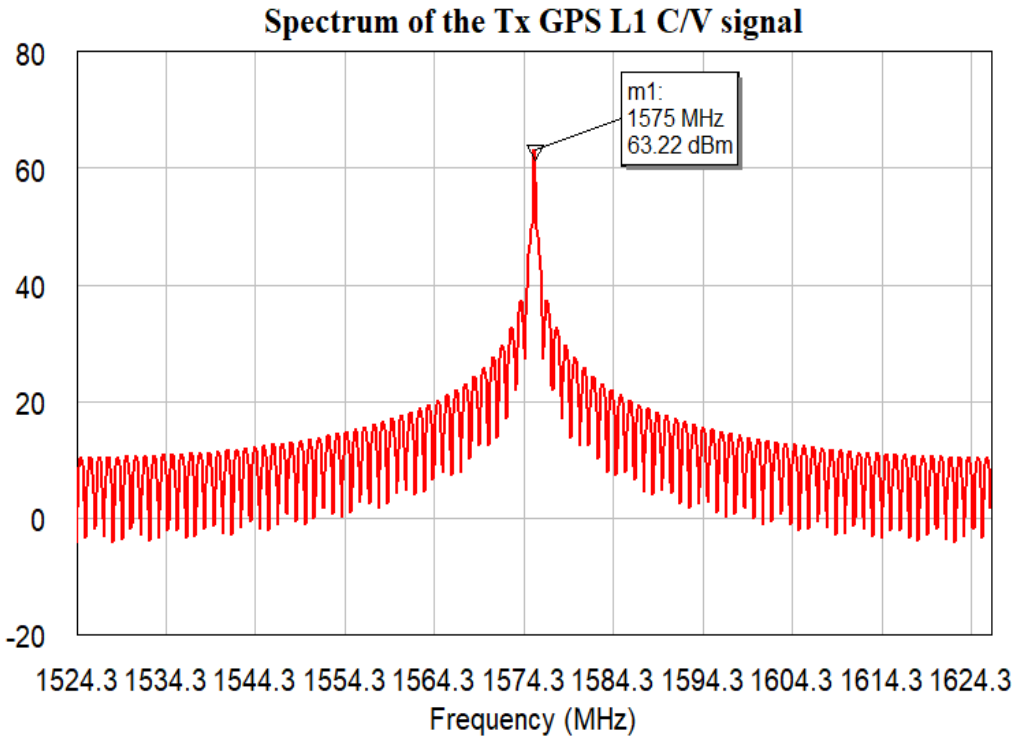

Figure 4.9 Transmitted GPS L1 C/V Signal

The transmitted signal travels a distance of 21000 km in free space to reach the receiver, thus loosing most of its power dropping to -160 dB when received, then it gets amplified in the first amplification stage (LNA+BGA1) with 47 dB of gain as demonstrated in Figure 4.10. The 1st stage of amplification is followed by a bandpass filter (SF1186B-2) for the GPS L1 C/V signal bandwidth, then to reach the full-scale voltage range of the ADC, a second amplification stage is added BGA2, BGA3 and VGA as shown in Figure 4.2. The output of the filtered and amplified GPS L1 signal is in Figure 4.11.

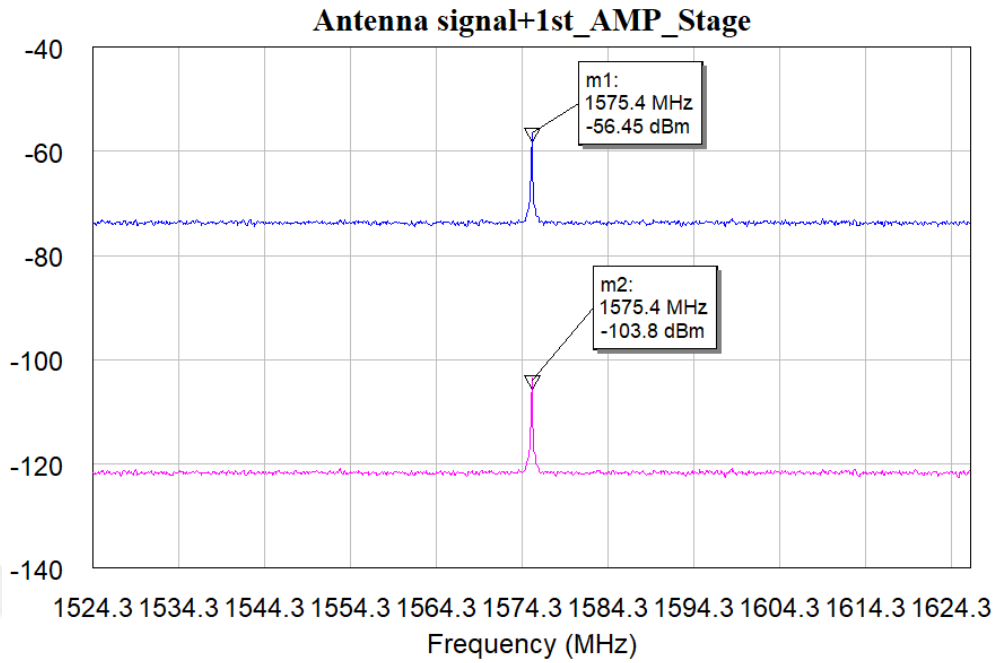

Figure 4.10 Received GPS L1 C/V Signal and after 1st stage amplification

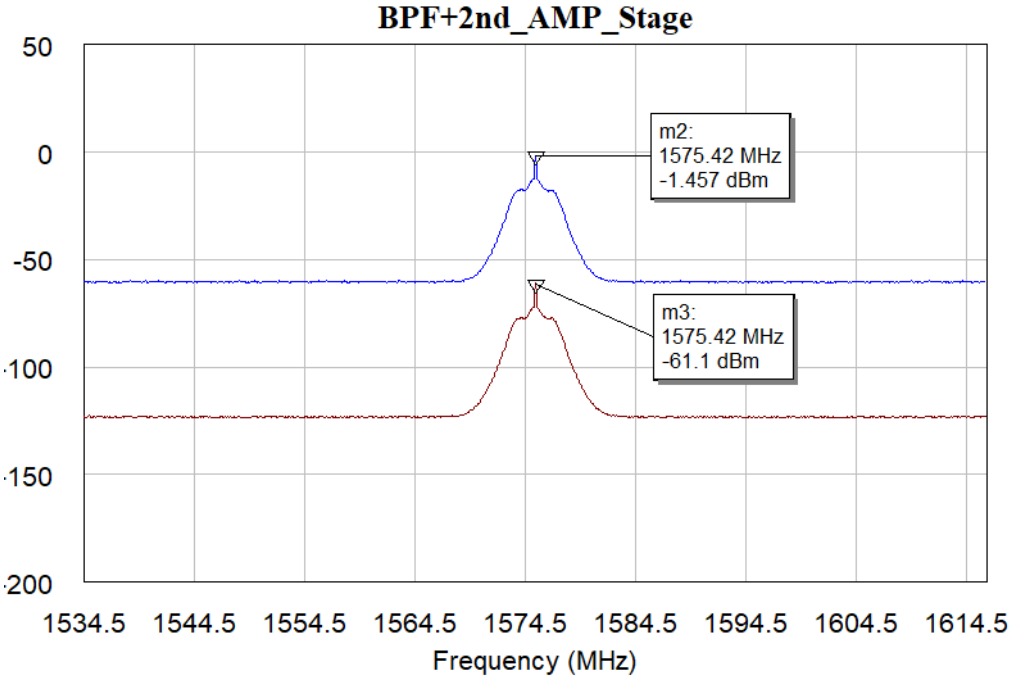

Figure 4.11 Filtered GPS L1 C/V Signal and after 2nd stage amplification

Figure 4.12 present the full power budget of the system that allow us to reach the full range scale of the ADC to reach the last stage which is sampling.

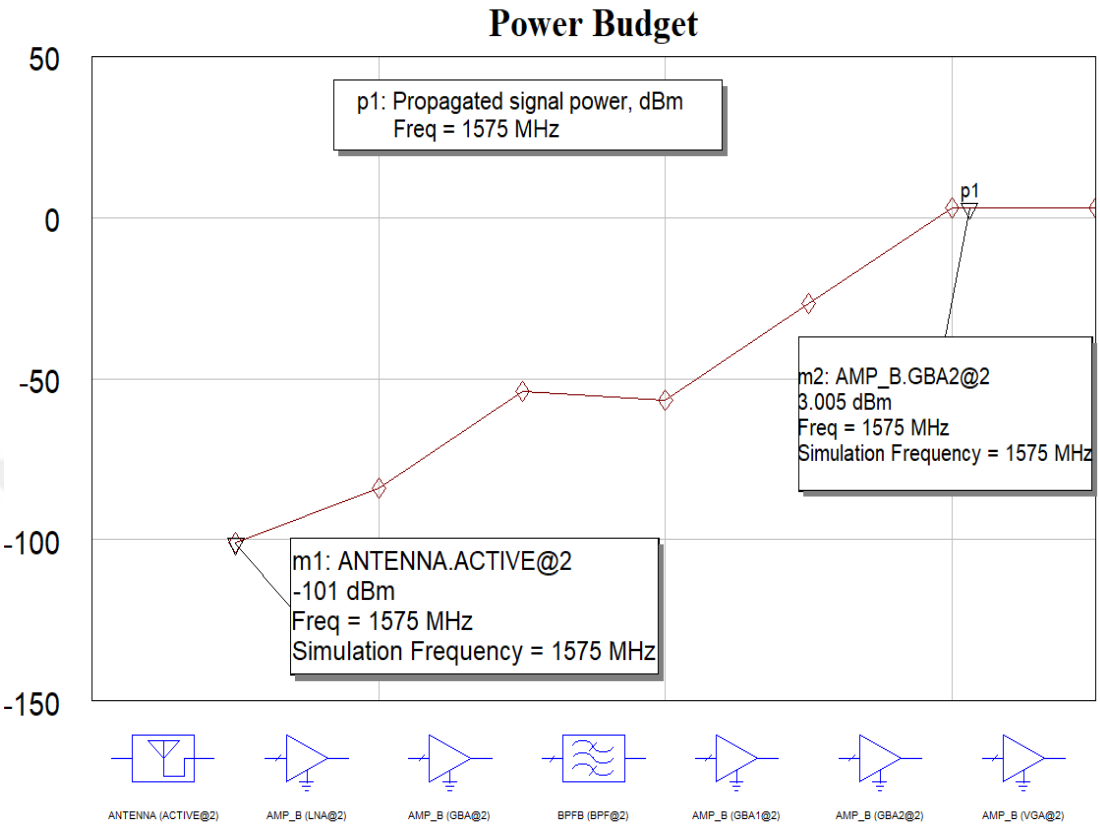

Figure 4.12 Front-end Power Budget

The last stage is the signal sampling, it starts with setting the ADC to several sampling frequencies obtained from the algorithm in section 3.9.1, the output graph below shows sampling done with 3 different sampling frequencies starting with sampling frequency $f_{s1} = 30.1217MHz$, $f_{s2} = 90.365\,MHz$, and $f_{s3} = 203.321MHz$.

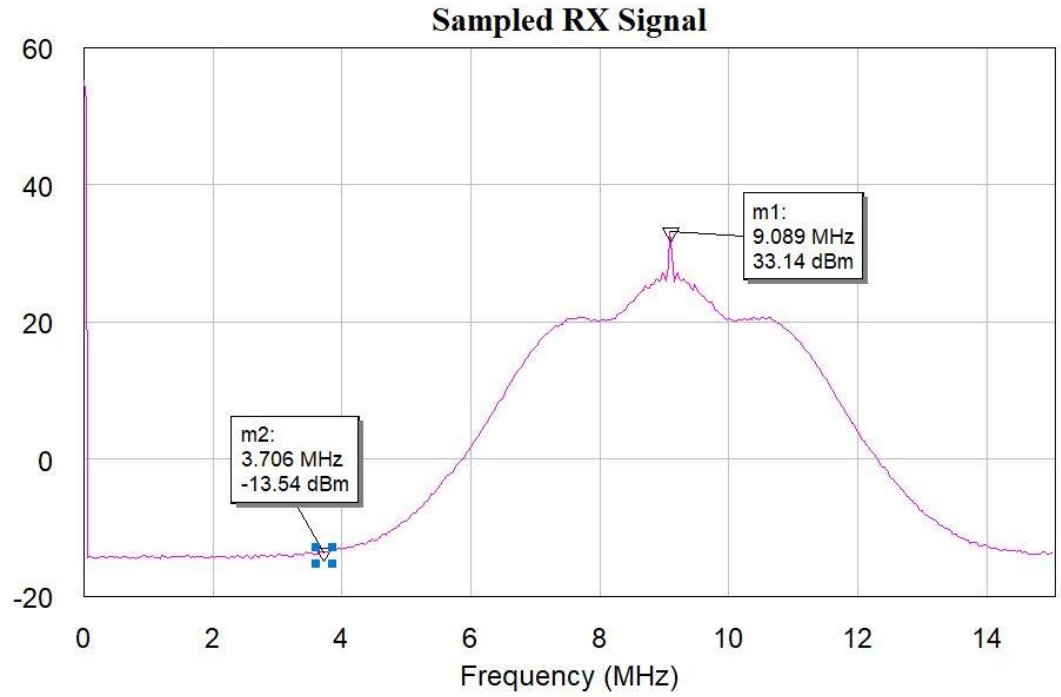

Figure 4.13 Sampled signal with $\boldsymbol{f_{s1} = 30.1217\ MHz}$

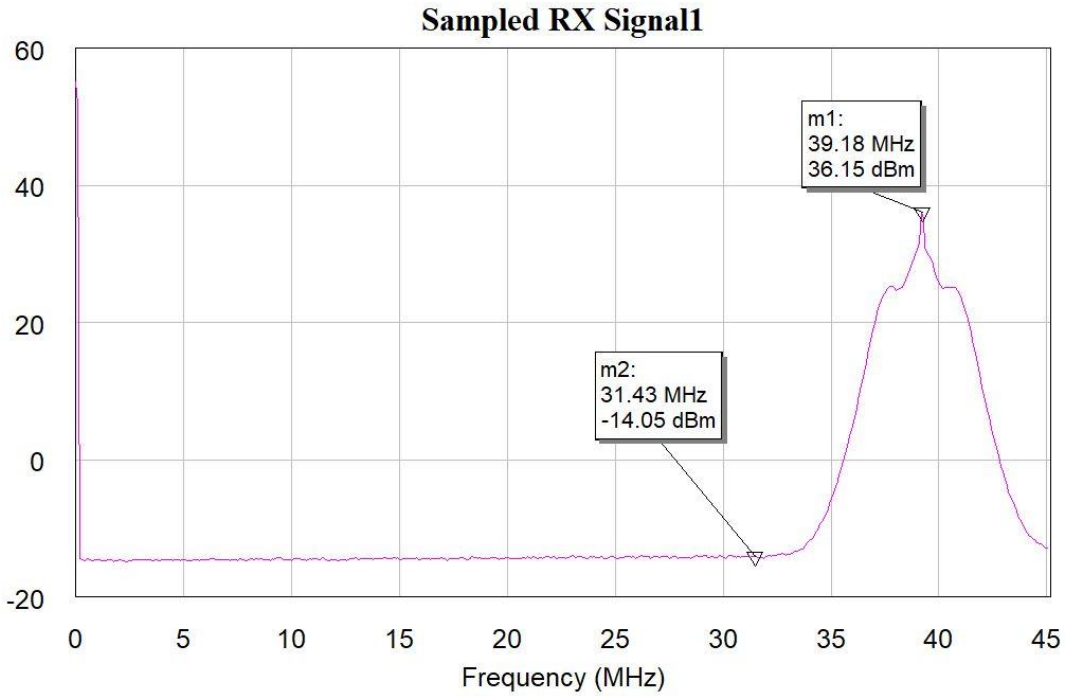

Figure 4.14 Sampled signal with $\boldsymbol{f_{s2} = 90.365\ MHz}$

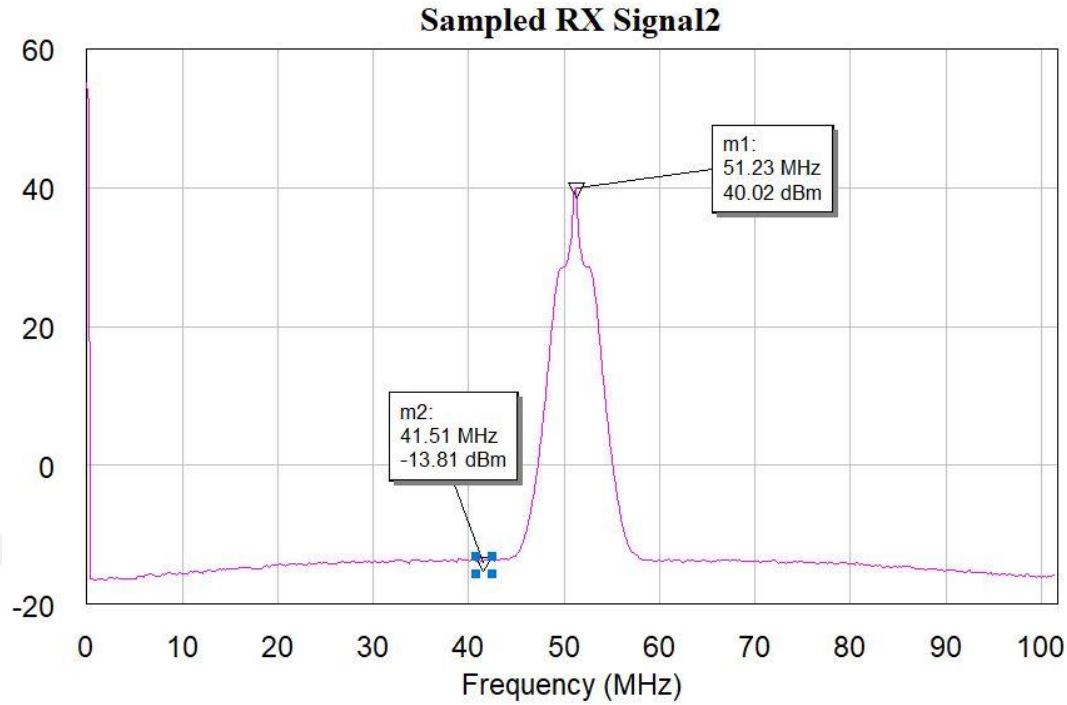

Figure 4.15 Sampled signal with $\boldsymbol{f_{s3} = 203.321\ MHz}$

As we can observe, each figure of the sampled signals presented doesn't have any interference with $\frac{f_s}{2}$, 0, and sampled signal from the negative spectrum which proves the concept of the algorithm in 3.9.1.

CHAPTER 5

DISCUSSION AND CONCLUSION

5.1 Conclusions and Future work

The recent development in the arena of global navigation satellite systems (GNSS) and the rise of available radio navigation signals has raised the problem that is the source of this research project. The traditional receiving front-ends of current GNSS receivers can become very complex when several distinct frequencies/bands are used. To overcome this complexity, the direct RF sampling (DRFS) architecture is proposed because it greatly reduces the hardware requirement in the traditional receiver by removing the mixer stages. The lack of theoretical contribution in the literature on the DRFS receiver is our main motive for presenting a complete DRFS receiver theoretical framework. This study tackled a few problems and presented feasible solutions to each one.

The first sub-problem raised the question of the feasibility of an RF signal processing chain (Front-end) broadband amplification while adding as little noise as possible. The solution related to this question is presented in 4.3 which explains the amplification required for such a processing chain. It was calculated that a gain of more than 100 dB is required to amplify the GNSS signals. Thus, successfully solving the first sub-problem.

The second sub-problem is the selection of the sampling frequency for single and multiple bands and its effects on noise folding and SNR. 3.9 proposed a new approach to implement simplified two sampling frequency selection algorithms on MATLAB with full completeness. The first algorithm is in the case of a single band (GPS L1 C/A) and calculates a minimum sampling frequency of $f_s = 30MHz$. The second one is in the case of multiple bands (GPS L1 C/A, GPS L2, GPS L5) and calculates a minimum sampling frequency of $f_s = 140MHz$. 3.9.3 added a full theoretical noise folding effects based on the sampling frequency. Thus, A successful solution to the second sub-problem.

After successfully solving these sub-problems, a complete GPS L1 C/A DRFS sampling receiver front-end has been simulated in the AWR design environment to correlate it with the complete theoretical framework presented. The simulation of the front-end amplifies the GPS L1 C/A by more than 100 dB. Then, several sampling frequencies selected by the algorithms (30.1217 MHz, 90.365 MHz, 203.321 MHz) are proved by the simulation, which shows no overlapping issues.

The results of this research represent an important step in the development of a universal multi-GNSS receiver. The findings allow us to move forward with the development of a hardware single-band receiver front-end and the possibility to design a multi-band GNSS receiver correlated with the simulation and theoretical framework presented, which will be able to capture all GNSS bands simultaneously. The efforts made will eventually lead to more accurate and reliable GNSS receivers for a multitude of consumer and professional applications.

In addition, although the designed receiver is applied to satellite navigation, the DRFS technique has a much broader scope, so some of the design methods in this dissertation can be extended to other domains. These include cellular telephony, wireless internet networks, satellite communications, etc., to name a few. Consumer technology products that aim to converge services are the most likely to benefit from DRFS because of the different frequencies used by these services. Advances in these areas will lead to smaller, lighter, and less expensive products.

REFERENCES

[1] Lechner, W., & Baumann, S.,"Global Navigation Satellite Systems - Education Curriculum" p. 52. 2012.

[2] Lamontagne, G., Landry, R. J., & Kouki, A. B. Direct RF Sampling GNSS Receiver Design and Jitter Analysis. Positioning, vol. 03, no. 04, pp. (46–61).2012.

[3] Akos, D. M., & Tsui, J. B. Y. Design and implementation of a direct digitization GPS receiver front end. IEEE Trans. Microw. Theory Tech., vol. 44, no. 12 PART 2, pp. (2334–2339).1996.

[4] Nguyen, A., Kisomi, A. A., & Landry, R. J. Avionic Systems applied to VOR and ILS. IEEE Radar Conference (RadarConf)., pp. (1622–1627). 2017.

[5] Bousseaud, P., Novakov, E., & Fournier, J. M. A direct RF signal sampling integrated receiver for IoT applications. Int. Conf. Adv. Technol. Commun., vol. 2016-Janua, pp. (237–242). 2016.

[6] Kaveh, A. Design and Fabrication of Multi-Band GNSS RF Front-End Receiver. Int. J. Signal Process. Image Process. Pattern Recognit., vol. 9, no. 4, pp. (47–60), Apr. 2016.

[7] Mahashreveta, C. What are various GNSS systems? – Geospatial World. Retrieved May 18, 2021, from https://www.geospatialworld.net/blogs/what-are-the-various-gnss-systems/.2019.

[8] U.S. government. GPS.gov: Space Segment.Retrieved Decmber 17, 2021, from https://www.gps.gov/systems/gps/space/.2021.

[9] Subirana, J., Zornoza, J., & Hernández-Pajares, M., "GNSS Data Processing", vol. II. 2013.

[10] Hossain, M. M. Design of RF Front End for Multi-Band Multi-System. GNSS p. 63. 2008.

[11] GMV. GPS Architecture.Retrieved May 18, 2021, from https://gssc.esa.int/navipedia/index.php/GPS_Architecture. 2011.

[12] Guidance, T., "The physics of GPS – Trilateration", STEM Learning. 2018.

[13] Sholarin, E. A. & Awange, J. L. Global navigation satellite system (GNSS). Environ. Sci. Eng. (Subseries Environ. Sci., no. 9783319276496, pp. (177–212). 2015.

[14] Paakki, T. Next Generation Multi-System Multi-Frequency GNSS Receivers. Tampere University of Technology, 2017.

[15] Karaim, M., Elsheikh, M., & Noureldin A. GNSS Error Sources. Multifunctional Operation and Application of GPS, IntechOpen. 2018.

[16] Lechner, W. & Baumann, S., "Global navigation satellite systems" Comput. Electron. Agric., vol. 25, no. 1–2, pp. (67–85). 2000.

[17] Blewitt, G., "Basics of the GPS Technique : Observation Equations,". 2000.

[18] Al Hares, K., & Majzoub, A. TDMA & FDMA Techniques. Grin Verlag. 2015.

[19] Sanz Subiran, J., Juan Zornoza, JM.,& Hernandez-Pajares, M. GPS Navigation Message - Navipedia.Retrieved May 18, 2021, From https://gssc.esa.int/navipedia/index.php/GPS_Navigation_Message. 2011.

[20] Enge, P. K. The Global Positioning System: Signals, measurements, and performance. Int. J. Wirel. Inf. Networks1, pp. (83–105), Apr. 1994.

[21] El-Rabbany, A., "Introduction to GPS: The Global Positioning System", Artech House.2002.

[22] Rodríguez, J. GPS Signal Plan. Retrieved Decmber 21, 2021,from https://gssc.esa.int/navipedia/index.php/GPS_Signal_Plan.2011.

[23] U.S. government. GPS.gov: New Civil Signals. Retrieved Decmber 21, 2021, from https://www.gps.gov/systems/gps/modernization/civilsignals/.2020.

[24] Betz, J. W., & Corporation, T. M. The Offset Carrier Modulation for GPS Modernization. Proceedings of the 1999 National Technical Meeting of The Institute of Navigation, pp. (639–648). 1998.

[25] DeMartino, C. The differences between Receiver Types, Part 2. Retrieved May 19, 2021, from https://www.mwrf.com/technologies/active-components/article/21846675/the-differences-between-receiver-types-part-2. 2016.

[26] Razavi, B., "RF Microelectronics", Pearson. (2nt Edition). 2011.

[27] Thor, J., & Akos, D. M. A direct RF sampling multifrequency GPS receiver. IEEE PLANS, Position Location and Navigation Symposium, pp. (44–51).2002.

[28] Li, X., & Ismail, M. Multi-Standard CMOS Wireless Receivers: Analysis and Design. Kluwer Academic Publishers. 2002.

[29] Tuttlebee, W. Software-defined radio: Facets of a developing technology. IEEE Pers. Commun., *vol. 6*, no. 2, pp. (38–44), Apr. 1999.

[30] Cruz, P., Gomes, H., & Carvalho N. Receiver Front-End Architectures – Analysis and Evaluation. *Advanced Microwave and Millimeter Wave*

Technologies Semiconductor Devices Circuits and Systems. pp.(1-10). InTech. 2010.

[31] "High-speed ADCs," 2021. https://www.ti.com/data-converters/adc-circuit/high-speed/rf-sampling.html#where.

[32] Neu, T. A checklist for designing RF-sampling receivers - EDN.Retrieved May 19, 2021, from https://www.edn.com/a-checklist-for-designing-rf-sampling-receivers/. 2016.

[33] Neu, T. Direct RF conversion: From vision to reality. *Texas Instruments White Pap.*pp.(1-8). 2015.

[34] Gomez, R. Theoretical Comparison of Direct-Sampling Versus Heterodyne RF Receivers. IEEE Trans. Circuits Syst. I Regul. Pap., *vol. 63*, no. 8, pp. (1276–1282), Aug. 2016.

[35] Frenzel, L. Fast ADC Facilitates Direct RF Sampling at Higher Frequencies. Retrieved May 19, 2021, from https://www.electronicdesign.com/technologies/analog/article/21805523/fast-adc-facilitates-direct-rf-sampling-at-higher-frequencies.

[36] Latiri, A., Joet, L., Desgreys, P., & Loumeau, P. A reconfigurable RF sampling receiver for multistandard applications. Comptes Rendus Physique, *vol. 7*, no. 7. 2006.

[37] Naik, M. R. & Vithalani, C. H. THE SOFTWARE-DEFINED RADIO IS NOW A REALITY. International Journal of Advanced Research in Electrical, pp.(1-4).2013.

[38] Miguel, J., & Nogueira, C. The Receiver Analysis and Design from a System Point of View, masters / doctoral dissertation, Technical University of Lisbon. 2013.

[39] Tektronix. Overview of Noise Measurements. pp. (1–63). 1998.

[40] Electronics-Notes. Understanding Radio Receiver Selectivity | Electronics Notes. Retrieved Sep. 07, 2021,from https://www.electronics-notes.com/articles/radio/radio-receiver-selectivity/basics.php. 2019.

[41] Tseng, C. H., & Chou, S. C. Direct downconversion of multiband RF signals using bandpass sampling. IEEE Trans. Wirel. Commun., *vol. 5*, no. 1, pp. (72–76). 2006.

[42] Psiaki, M. L., Akos, D. M., & Thor, J. A comparison of direct radio frequency sampling and conventional GNSS receiver architectures. Navig. J. Inst. Navig., vol. 52, no. 2, pp. (71–81). 2005.

[43] Psiaki, M. L., Powell, S. P., Jung, H., & Kintner, P. M. Design and practical implementation of multifrequency RF front ends using direct RF sampling.

IEEE Trans. Microw. Theory Tech., *vol. 53*, no. 10, pp. (3082–3089). 2005.

[44] Liu, J. C. Complex bandpass sampling and direct downconversion of multiband analytic signals. Signal Processing, *vol. 90*, no. 2, pp. (504–512). 2010.

[45] Li, W., & Liu, Z. A bandpass sampling design in multi-channel radio Receiver. Procedia Environ. Sci., *vol. 11*, no. PART A, pp. (250–255). 2011.

[46] Akos, D. M., Stockmaster, M., Tsui, J. B. Y., & Caschera, J. Direct bandpass sampling of multiple distinct RF signals. IEEE Trans. Commun., *vol. 47*, no. 7, pp.(983–988).1999.

[47] Lyons, R. G. , " *Understanding Digital Signal Processing- Second Edition*",. Prentice Hall PIR. 2004.

[48] Choe, M., & Kim, K. Bandpass sampling algorithm with normal and inverse placements for multiple RF signals. IEICE Trans. Commun., *vol. E88-B*, no. 2, pp. (754–757), 2005.

[49] Mookiah, V. Quadrature BandPass Sampling Front-end for Global Navigation Satellite Systems, masters / doctoral dissertation, The University of New South Wales. 2015.

[50] Li, Y. Design of High Speed Folding and Interpolating Analog-To-Digital Converter, masters / doctoral dissertation, Texas A&M University.2003.

[51] Lizon, B., Hall, C., Andrews, R., & Wuerker, J., "Fundamentals of Precision ADC Noise Analysis", All About Circuits,p. 65. 2020.

[52] Syrjälä, V., Valkama, M., & Renfors, M. Design considerations for direct RF sampling receiver in GNSS environment. 5th Work. Positioning, Navig. Commun., pp. (9–13). 2008.

[53] Barrett, C. Fractional/integer-N PLL basics. Texas Instruments,p. 55. 1999.

[54] Dempster, A. Aperture Jitter Effects in Software Radio GNSS Receivers. J. Glob. Position. Syst., vol. 3, no. 1&2, pp. (45–48). 2004.

CURRICULUM VITAE

PERSONAL INFORMATION

Name Surname: AHMED ELTAYEB AHMED ELBUSHRA

Nationality: Sudanese

Phone :

E-mail:

EDUCATION

High School: Saudi Arabian School In Ankara – Ankara, turkey, (Sep 2011 - Jun 2014) with (CGPA 98.81%).

Bachelor: B.Sc. in Electrical and electronics Engineering- Faculty of Engineering and Natural Sciences- Ankara Yildirim Beyazit University- Ankara, turkey, (Sep 2014 - Jun 2019) with (CGPA 80.25%).

Master's degree: M.Sc. in Electrical and electronics Engineering - Faculty of Engineering and Natural Sciences - Ankara Yildirim Beyazit University, Ankara,turkey (2019 - 2023) with (CGPA 95.25%).

PUBLICATIONS

WORK EXPERIENCE

- An intern in Turkish Radio and Television Corporation, Jul 2015 - Aug 2015.
- An intern in GAYDA ENERJİ MÜHENDİSLİK BİLİŞİM SAN. TİC. LTD. ŞTİ, Jun 2018- Aug 2018.
- A Researcher in EHSİM Elektronik Harp Sistemleri Müh. Tic. A.Ş., Jul 2020 – 2022.

TOPICS OF INTEREST

- Telecommunications.
- GNSS system.
- RF design.
- Microcontrollers.